

# Properties of rotating Einstein-Maxwell-Dilaton black holes in odd dimensions

**Jose Luis Blázquez-Salcedo<sup>1</sup>, Jutta Kunz<sup>2</sup>, Francisco Navarro-Lérida<sup>3</sup>**

<sup>1</sup> Dept. de Física Teórica II, Ciencias Físicas

Universidad Complutense de Madrid, E-28040 Madrid, Spain

<sup>2</sup> Institut für Physik, Universität Oldenburg

Postfach 2503, D-26111 Oldenburg, Germany

<sup>3</sup> Dept. de Física Atómica, Molecular y Nuclear, Ciencias Físicas

Universidad Complutense de Madrid, E-28040 Madrid, Spain

April 2, 2024

## Abstract

We investigate rotating Einstein-Maxwell-Dilaton (EMd) black holes in odd dimensions. Focusing on black holes with equal-magnitude angular momenta, we determine the domain of existence of these black holes. Non-extremal black holes reside with the boundaries determined by the static and the extremal rotating black holes. The extremal EMd black holes show proportionality of their horizon area and their angular momenta. Thus the charge does not enter. We also address the Einstein-Maxwell case, where the extremal rotating black holes exhibit two branches. On the branch emerging from the Myers-Perry solutions their angular momenta are proportional to their horizon area, whereas on the branch emerging from the static solutions their angular momenta are proportional to their horizon angular momenta. Only subsets of the near-horizon solutions are realized globally. Investigating the physical properties of these EMd black holes, we note that one can learn much about the extremal rotating solutions from the much simpler static solutions. The angular momenta of the extremal black holes are proportional to the area of the static ones for the Kaluza-Klein value of the dilaton coupling constant, and remain analogous for other values. The same is found for the horizon angular velocities of the extremal black holes, which possess an analogous behavior to the surface gravity of the static black holes. The gyromagnetic ratio is rather well approximated by the ‘static’ value, obtained perturbatively for small angular momenta.

# 1 Introduction

Discovered in 1986 by Myers and Perry (MP) [1, 2], the rotating higher-dimensional vacuum black holes have been generalized to include various types of matter fields (see e.g. [3, 4, 5]), as motivated by supergravity and string theory. New analytical black hole solutions can be obtained by a number of solution generation techniques. A straightforward method is based on the Kaluza-Klein (KK) reduction. In the simplest case this leads to electrically charged Einstein-Maxwell-dilaton (EMd) black holes for a particular value of the dilaton coupling constant,  $h = h_{\text{KK}}$  [6, 7, 8, 9]. For general dilaton coupling constant  $h$ , however, rotating EMd black hole solutions or their Einstein-Maxwell (EM) counterparts need either perturbative techniques [10, 11, 12, 13, 14, 15, 16] or numerical analysis [17, 18, 19].

General stationary black holes in  $D$  dimensions possess  $N = [(D-1)/2]$  independent angular momenta  $J_i$ , associated with  $N$  orthogonal planes of rotation [1], where  $N$  is the integer part of  $(D-1)/2$ , corresponding to the rank of the rotation group  $SO(D-1)$ . In odd- $D$  dimensions, when all  $N$  angular momenta have equal-magnitude, the symmetry of the solutions is enhanced. The EMd equations then simplify, leading to cohomogeneity-1 equations.

Here we consider such cohomogeneity-1 EMd black holes. On the one hand, we solve the coupled system of EMd equations numerically and study the properties of the black holes both for extremal and non-extremal solutions. On the other hand, we derive the near-horizon solutions for the extremal black holes. The physical properties of non-extremal black holes, like the horizon area, the gyromagnetic ratio, or the surface gravity then assume values that are bounded by those of the extremal black holes and those of the static black holes.

For extremal MP black holes in odd- $D$  dimensions the horizon area  $A_{\text{H}}$  is proportional to the magnitude of the equal angular momenta,  $J = |J_i|$ ,  $J = \sqrt{2(D-3)}A_{\text{H}}$ . This relation for extremal black holes represents the limiting case of a more general relation for MP black holes in terms of the inner and outer horizon areas of non-extremal black holes [20], and was pointed out in four dimensions before [21, 22, 23, 24, 25, 26, 27]. In the presence of charge, the relation generalizes, and the product of the horizon areas can typically be written as a sum between the squares of the angular momenta and some powers of the charges [20, 21, 22, 23, 24, 25, 26, 27, 28]. Area-angular momentum-charge inequalities for stable marginally outer trapped surfaces were studied for EMd theory in [29, 30].

Considering such area-angular momentum relations for extremal EMd and EM black holes, we find that the EM case is special, since there are two branches of extremal solutions. The first branch emerges from the MP black holes and retains the proportionality between angular momentum and area. Thus the charge does not enter here. The second branch emerges from the higher-dimensional Reissner-Nordström (RN) black holes. Here the proportionality between angular momentum and area is lost. Instead there is a new proportionality between angular momentum and horizon angular momentum along this second branch. As soon as the dilaton is coupled, however, the second branch

disappears and the proportionality between angular momentum and area persists for all extremal EMD solutions, independent of the dilaton coupling constant  $h$ .

The paper is organized as follows. In section 2 we present the action, the parametrization for the metric and the fields, as well as the general formulae for the physical properties. In section 3 we briefly recall the analytically known Kaluza-Klein black holes and their properties. We derive the near-horizon solutions in section 4, discussing in particular, the two-branch structure in the EM case. Section 5 contains our numerical results. Here we exhibit the properties of five-dimensional black holes in detail, and demonstrate subsequently, that the pattern observed in five dimensions is generic for higher dimensions. We present our conclusions in section 6.

## 2 Action, Ansätze and Charges

### 2.1 Einstein-Maxwell-dilaton action

We consider the  $D$ -dimensional EMD action

$$I = \int d^D x \sqrt{-g} \left[ R - \frac{1}{2} \partial_\mu \phi \partial^\mu \phi - \frac{1}{4} e^{-2h\phi} F_{\mu\nu} F^{\mu\nu} \right], \quad (1)$$

with curvature scalar  $R$ , dilaton field  $\phi$ , dilaton coupling constant  $h$ , and field strength tensor  $F_{\mu\nu} = \partial_\mu A_\nu - \partial_\nu A_\mu$ , where  $A_\mu$  denotes the gauge potential. We choose units such that  $16\pi G_D = 1$ , where  $G_D$  is the  $D$ -dimensional Newton constant.

Variation of the action with respect to the metric leads to the Einstein equations

$$R_{\mu\nu} - \frac{1}{2} g_{\mu\nu} R = \frac{1}{2} T_{\mu\nu}, \quad (2)$$

with stress-energy tensor

$$T_{\mu\nu} = \partial_\mu \phi \partial_\nu \phi - \frac{1}{2} g_{\mu\nu} \partial_\rho \phi \partial^\rho \phi + e^{-2h\phi} \left( F_{\mu\rho} F_\nu{}^\rho - \frac{1}{4} g_{\mu\nu} F_{\rho\sigma} F^{\rho\sigma} \right), \quad (3)$$

whereas variation with respect to the fields yields for the Maxwell field

$$\nabla_\mu \left( e^{-2h\phi} F^{\mu\nu} \right) = 0, \quad (4)$$

and for the dilaton field

$$\nabla_\mu \nabla^\mu \phi = -\frac{h}{2} e^{-2h\phi} F_{\mu\nu} F^{\mu\nu}. \quad (5)$$

Special cases correspond to Einstein-Maxwell theory, where  $h = 0$ , and to Kaluza-Klein theory, where  $h = h_{\text{KK}}$ ,

$$h_{\text{KK}} = \sqrt{\frac{D-1}{2(D-2)}}. \quad (6)$$

## 2.2 Ansätze

To obtain stationary black hole solutions, which represent generalizations of the Myers-Perry solutions [1] to EMD theory, we consider black hole spacetimes with  $N$ -azimuthal symmetries, implying the existence of  $N + 1$  commuting Killing vectors,

$$\xi \equiv \partial_t, \quad \eta_{(k)} \equiv \partial_{\varphi_k}, \quad (7)$$

for  $k = 1, \dots, N$ . Hence we are considering black holes with spherical horizon topology.

While the general EMD black holes possess  $N$  independent angular momenta, we now restrict to black holes whose angular momenta have all equal-magnitude. In odd dimensions, the metric and the gauge field parametrization then simplify considerably, and the problem reduces to cohomogeneity-1. The EMD equations then form a set of ordinary differential equations, just as in Einstein-Maxwell theory [18].

We parametrize the metric as follows [17, 18]

$$\begin{aligned} ds^2 = & -f dt^2 + \frac{m}{f} \left[ dr^2 + r^2 \sum_{i=1}^{N-1} \left( \prod_{j=0}^{i-1} \cos^2 \theta_j \right) d\theta_i^2 \right] \\ & + \frac{n}{f} r^2 \sum_{i=1}^N \left( \prod_{j=0}^{i-1} \cos^2 \theta_j \right) \sin^2 \theta_i \left( \varepsilon_i d\varphi_i - \frac{\omega}{r} dt \right)^2 \\ & + \frac{m-n}{f} r^2 \left\{ \sum_{i=1}^N \left( \prod_{j=0}^{i-1} \cos^2 \theta_j \right) \sin^2 \theta_i d\varphi_i^2 \right. \\ & \left. - \left[ \sum_{i=1}^N \left( \prod_{j=0}^{i-1} \cos^2 \theta_j \right) \sin^2 \theta_i \varepsilon_i d\varphi_i \right]^2 \right\}, \end{aligned} \quad (8)$$

where  $\theta_0 \equiv 0$ ,  $\theta_i \in [0, \pi/2]$  for  $i = 1, \dots, N-1$ ,  $\theta_N \equiv \pi/2$ ,  $\varphi_k \in [0, 2\pi]$  for  $k = 1, \dots, N$ , and  $\varepsilon_k = \pm 1$  denotes the sense of rotation in the  $k$ -th orthogonal plane of rotation.

An adequate parametrization for the gauge potential is given by

$$A_\mu dx^\mu = a_0 dt + a_\varphi \sum_{i=1}^N \left( \prod_{j=0}^{i-1} \cos^2 \theta_j \right) \sin^2 \theta_i \varepsilon_i d\varphi_i. \quad (9)$$

Independent of the number of dimensions  $D$ , this parametrization involves four functions for the metric,  $f$ ,  $m$ ,  $n$ ,  $\omega$ , two functions for the gauge field,  $a_0$ ,  $a_\varphi$ , and one function for the dilaton field,  $\phi$ , all of which depend only on the radial coordinate  $r$ .

## 2.3 Global charges

We consider asymptotically flat solutions. Thus, asymptotically the metric should approach the Minkowski metric.

The mass  $M$  and the angular momenta  $J_{(k)}$  of the black holes are obtained from the Komar expressions associated with the respective Killing vector fields

$$M = -\frac{D-2}{D-3} \int_{S_\infty^{D-2}} \alpha , \quad (10)$$

$$J_{(k)} = \int_{S_\infty^{D-2}} \beta_{(k)} , \quad (11)$$

where  $\alpha_{\mu_1 \dots \mu_{D-2}} \equiv \epsilon_{\mu_1 \dots \mu_{D-2} \rho \sigma} \nabla^\rho \xi^\sigma$ , and  $\beta_{(k) \mu_1 \dots \mu_{D-2}} \equiv \epsilon_{\mu_1 \dots \mu_{D-2} \rho \sigma} \nabla^\rho \eta_{(k)}^\sigma$ . Equal-magnitude angular momenta then satisfy  $|J_{(k)}| = J$ ,  $k = 1, \dots, N$ .

The electric charge  $Q$  is obtained from

$$Q = -\frac{1}{2} \int_{S_\infty^{D-2}} e^{-2h\phi} {}^*F , \quad (12)$$

with  ${}^*F_{\mu_1 \dots \mu_{D-2}} \equiv \epsilon_{\mu_1 \dots \mu_{D-2} \rho \sigma} F^{\rho \sigma}$ . The magnetic moment  $\mu_{\text{mag}}$  is determined from the asymptotic expansion of the gauge potential  $a_\varphi$ . The gyromagnetic ratio  $g$  is then obtained from the magnetic moment  $\mu_{\text{mag}}$  via

$$\mu_{\text{mag}} = g \frac{QJ}{2M} . \quad (13)$$

The dilaton charge  $\Sigma$  is defined via

$$\Sigma = -A(S^{D-2}) \lim_{r \rightarrow \infty} r^{D-2} \frac{d\phi}{dr} , \quad (14)$$

where  $A(S^{D-2})$  is the area of the  $S^{D-2}$  sphere.

## 2.4 Horizon properties

The event horizon is located at  $r = r_{\text{H}}$ . Here the Killing vector  $\chi$ ,

$$\chi = \xi + \Omega \sum_{k=1}^N \varepsilon_k \eta_{(k)} , \quad (15)$$

is null, and  $\Omega$  represents the horizon angular velocity. Without loss of generality,  $\Omega$  is assumed to be non-negative, any negative sign being included in  $\varepsilon_k$ .

The area of the horizon  $A_{\text{H}}$  is given by

$$A_{\text{H}} = \int_{\mathcal{H}} \sqrt{|g^{(D-2)}|} = r_{\text{H}}^{D-2} A(S^{D-2}) \lim_{r \rightarrow r_{\text{H}}} \sqrt{\frac{m^{D-3} n}{f^{D-2}}} , \quad (16)$$

and the surface gravity  $\kappa$  reads

$$\kappa^2 = -\frac{1}{2} (\nabla_\mu \chi_\nu) (\nabla^\mu \chi^\nu) \Big|_{\mathcal{H}} = \lim_{r \rightarrow r_{\text{H}}} \frac{f}{(r - r_{\text{H}}) \sqrt{m}} . \quad (17)$$

The horizon mass  $M_{\text{H}}$  and horizon angular momenta  $J_{\text{H}(k)}$  are given by

$$M_{\text{H}} = -\frac{D-2}{D-3} \int_{\mathcal{H}} \alpha , \quad (18)$$

$$J_{\text{H}(k)} = \int_{\mathcal{H}} \beta_{(k)} , \quad (19)$$

where  $\mathcal{H}$  represents the surface of the horizon. For equal-magnitude angular momenta  $|J_{\text{H}(k)}| = J_{\text{H}}$ ,  $k = 1, \dots, N$ .

The electric charge  $Q$  can also be determined at the horizon via

$$Q = -\frac{1}{2} \int_{\mathcal{H}} e^{-2h\phi} {}^*F . \quad (20)$$

The horizon electrostatic potential  $\Phi_{\text{H}}$  is defined by

$$\Phi_{\text{H}} = \chi^\mu A_\mu|_{r=r_{\text{H}}} . \quad (21)$$

$\Phi_{\text{H}}$  is constant at the horizon.

## 2.5 Mass formula

The Smarr mass formula for Einstein-Maxwell black holes with  $N$  equal-magnitude angular momenta reads [17, 31]

$$\frac{D-3}{D-2} M = 2\kappa A_{\text{H}} + N\Omega J + \frac{D-3}{D-2} \Phi_{\text{H}} Q . \quad (22)$$

This mass formula holds also in the presence of a dilaton field [9].

Introducing the dilaton charge into the mass formula via [9]

$$\frac{\Sigma}{h} = -\Phi_{\text{H}} Q , \quad (23)$$

Eq. (22) yields the Smarr mass formula

$$M = 2\frac{D-2}{D-3} \kappa A_{\text{H}} + \frac{D-2}{D-3} N\Omega J + 2\Phi_{\text{H}} Q + \frac{\Sigma}{h} , \quad (24)$$

known to hold also for non-Abelian black holes (in  $D = 4$ ) [32].

## 2.6 Scaling symmetry

We note that the solutions have a scaling symmetry, e.g.,

$$\tilde{M} = \tau^{D-3} M \quad \tilde{J}_i = \tau^{D-2} J_i \quad \tilde{Q} = \tau^{D-3} Q , \quad (25)$$

$$\tilde{r}_{\text{H}} = \tau r_{\text{H}} , \quad \tilde{\Omega} = \Omega/\tau , \quad \tilde{\kappa} = \kappa/\tau , \quad (26)$$

etc.

Let us therefore introduce scaled quantities, where we scale with respect to appropriate powers of the mass. These scaled quantities include the scaled angular momentum  $j = |J|/M^{(D-2)/(D-3)}$ , the scaled charge  $q = |Q|/M$ , the scaled area  $a_H = A_H/M^{(D-2)/(D-3)}$ , the scaled surface gravity  $\bar{\kappa} = \kappa M^{1/(D-3)}$ , and the scaled horizon angular velocity  $\bar{\Omega} = \Omega M^{1/(D-3)}$ .

In terms of the scaled quantities, the Smarr relation Eq. (22) reads

$$1 = 2 \frac{D-2}{D-3} \bar{\kappa} a_H + \frac{D-2}{D-3} N \bar{\Omega} j + \Phi_H q . \quad (27)$$

### 3 Kaluza-Klein black holes

A straightforward method to obtain charged rotating black hole solutions in  $D$  dimensions is based on the Kaluza-Klein reduction. Here one embeds a  $D$ -dimensional vacuum solution in  $D+1$  dimensions, performs a boost transformation, and then reduces the solution to  $D$  dimensions [6, 7, 8, 33, 9].

The KK black holes, obtained in this way for the particular value of the dilaton coupling constant  $h = h_{\text{KK}}$ ,

$$h_{\text{KK}} = \frac{D-1}{\sqrt{2(D-1)(D-2)}} = (D-1)\iota , \quad (28)$$

also satisfy the quadratic relation [34, 35, 9]

$$\frac{Q^2}{M - \frac{2(D-2)\iota}{D-3}\Sigma} = -2(D-3)\iota\Sigma . \quad (29)$$

This relation determines the dilaton charge in terms of the mass and the electric charge, while the angular momenta do not enter.

In contrast, the static black hole solutions are known analytically for arbitrary value of the dilaton coupling constant [36, 37, 38]. It should be interesting to find a generalization of relation Eq. (29) for general values of the coupling constant  $h$ .

#### 3.1 Physical properties

Let us briefly recall some properties of these KK black holes. In terms of parameters  $m$ ,  $a_i$ , and  $\alpha$ , their mass  $M$ , angular momenta  $J_i$ , charge  $Q$ , magnetic momenta  $\mu_{\text{mag},i}$ , and dilaton charge  $\Sigma$  are given by

$$M = m \left( 1 + (D-3) \cosh^2 \alpha \right) A(S^{D-2}) , \quad (30)$$

$$J_i = 2m a_i \cosh \alpha A(S^{D-2}) , \quad (31)$$

$$Q = (D - 3)m \sinh \alpha \cosh \alpha A(S^{D-2}) , \quad (32)$$

$$\mu_{\text{mag},i} = (D - 3)m a_i \sinh \alpha A(S^{D-2}) , \quad (33)$$

$$\Sigma = -\frac{(D - 3)m \sinh^2 \alpha}{2(D - 2)\iota} A(S^{D-2}) , \quad (34)$$

where  $m$  and  $a_i$  determine the MP mass and angular momenta in the limit, where the boost parameter vanishes,  $\alpha = 0$ .

The gyromagnetic ratios  $g_i$  are given by

$$g_i = \frac{2M}{QJ_i} \mu_{\text{mag},i} = (D - 3) + \frac{1}{\cosh^2 \alpha} \equiv g . \quad (35)$$

Thus the gyromagnetic ratio  $g$  depends only on the charge-to-mass ratio,  $q = Q/M$ . It does not depend on the angular momenta. Therefore, for a given value of  $q$ , the gyromagnetic ratio is the same for all rotating black holes. It ranges between  $g = D - 2$  in the limit of vanishing charge,  $q \rightarrow 0$ , and  $g = D - 3$  in the limit of maximal charge,  $|q| \rightarrow 1$ .

The event horizon of the KK black holes is characterized as the largest non-negative root  $\rho = \rho_{\text{H}}$  of

$$\Delta \equiv \prod_{i=1}^N (\rho^2 + a_i^2) - m \rho^{2-\varepsilon} , \quad (36)$$

where  $\varepsilon$  takes the values  $\varepsilon = 0, 1$  for odd and even dimensions, respectively. Notice that  $\rho$  is a Boyer-Lindquist type of radial coordinate. The (constant) horizon angular velocities  $\Omega_i$ , the horizon area  $A_{\text{H}}$ , the surface gravity  $\kappa$ , and the horizon electrostatic potential  $\Phi_{\text{H}}$  are given by

$$\Omega_i = \frac{a_i}{(\rho_{\text{H}}^2 + a_i^2) \cosh \alpha} , \quad (37)$$

$$A_{\text{H}} = \frac{\cosh \alpha}{\rho_{\text{H}}^{1-\varepsilon}} A(S^{D-2}) \prod_{i=1}^N (\rho_{\text{H}}^2 + a_i^2) , \quad (38)$$

$$\kappa = \left. \frac{\Delta_{,\rho}}{2m \rho_{\text{H}}^{2-\varepsilon} \cosh \alpha} \right|_{\rho=\rho_{\text{H}}} , \quad (39)$$

$$\Phi_{\text{H}} = \frac{\sinh \alpha}{\cosh \alpha} . \quad (40)$$

Thus, like  $g$ , the horizon electrostatic potential  $\Phi_{\text{H}}$  depends only on the charge-to-mass ratio  $q$ , with  $0 \leq \Phi_{\text{H}} \leq 1$ .

These KK black holes satisfy the general Smarr formula

$$M = 2 \frac{D-2}{D-3} \kappa A_{\text{H}} + \frac{D-2}{D-3} \sum_{i=1}^N \Omega_i J_i + \Phi_{\text{H}} Q , \quad (41)$$

which also holds for arbitrary dilaton coupling constant  $h$ .



### 3.2 Extremal solutions

We now turn to the extremal rotating KK black holes. We focus on black holes with equal-magnitude angular momenta,  $J_i = J$ ,  $i = 1, \dots, N$ . First, we present the metric

$$ds^2 = \left(1 + \frac{m \sinh^2 \alpha}{\rho^\varepsilon (\rho^2 + a^2)^{N-1}}\right)^{\frac{1}{D-2}} \left\{ -dt^2 + \frac{\rho^2 (\rho^2 + a^2)^{N-1}}{(\rho^2 + a^2)^N - m \rho^{2-\varepsilon}} d\rho^2 \right. \\ \left. + (\rho^2 + a^2) \sum_{i=1}^N (d\mu_i^2 + \mu_i^2 d\phi_i^2) + \varepsilon \rho^2 d\nu^2 + \frac{m \left( \cosh^2 \alpha dt - a \sum_{i=1}^N \mu_i^2 d\phi_i \right)^2}{\rho^\varepsilon (\rho^2 + a^2)^{N-1} + m \sinh^2 \alpha} \right\} \quad (42)$$

where  $\mu_i$ , the direction cosines, can be chosen in odd  $D$ -dimensions

$$\mu_i = \sin \theta_i \prod_{j=0}^{i-1} \cos \theta_j, \quad (43)$$

where  $\theta_0 = 0$ ,  $\theta_N = \pi/2$ , and in even  $D$ -dimensions

$$\mu_i = \sin \theta_{(i+1)} \prod_{j=0}^i \cos \theta_j, \quad (44)$$

where  $\theta_0 = 0$ ,  $\theta_{N+1} = \pi/2$ , and  $\mu_0 = \nu$ . Note that  $\sum_{i=1}^N \mu_i^2 + \varepsilon \nu^2 = 1$ .

The gauge potential is given by

$$A = \frac{m \sinh \alpha}{\rho^\varepsilon (\rho^2 + a^2)^{N-1} + m \sinh^2 \alpha} \left( \cosh^2 \alpha dt - a \sum_{i=1}^N \mu_i d\phi_i \right). \quad (45)$$

Finally, the dilaton is given by the following expression

$$\phi = -\frac{D-1}{2(D-2)} \log \left( 1 + \frac{m \sinh^2 \alpha}{\rho^\varepsilon (\rho^2 + a^2)^{N-1}} \right). \quad (46)$$

These extremal black holes are characterized only by two free parameters, since the angular momentum parameter  $a$  and the mass parameter  $m$  can be given in terms of the horizon radius  $\rho_H$ :

$$\begin{aligned} \text{even } D : \quad & a^2 = (2N-1) \rho_H^2, \\ & m = (2N)^N \rho_H^{2N-1}, \\ \text{odd } D : \quad & a^2 = (N-1) \rho_H^2, \\ & m = N^N \rho_H^{2N-2}. \end{aligned} \quad (47)$$

The relation between area and angular momentum for extremal black holes then follows

$$\begin{aligned} \text{even } D : \quad & J = 2\sqrt{D-3}A_{\text{H}} , \\ \text{odd } D : \quad & J = \sqrt{2(D-3)}A_{\text{H}} . \end{aligned} \quad (48)$$

Considering the Smarr relation Eq. (22), we note that on the one hand for extremal black holes we have vanishing  $\bar{\kappa}$ , thus

$$1 = \frac{D-2}{D-3} N \bar{\Omega} j \Big|_{\text{ex}} + \Phi_{\text{H}} q . \quad (49)$$

On the other hand, for static black holes we have vanishing  $\bar{\Omega}$ , thus

$$1 = 2 \frac{D-2}{D-3} \bar{\kappa} a_{\text{H}} \Big|_{\text{st}} + \Phi_{\text{H}} q . \quad (50)$$

Since the horizon electrostatic potential  $\Phi_{\text{H}}$  is independent of the angular momentum, we obtain for a given  $q$  the interesting relation

$$N \bar{\Omega} j \Big|_{\text{ex}} = 2 \bar{\kappa} a_{\text{H}} \Big|_{\text{st}} . \quad (51)$$

The scaled area  $a_{\text{H}}$  of the static solutions is proportional to the scaled angular momenta  $j$  of the extremal solutions, coinciding in five dimensions. For odd dimensions we find

$$j_{\text{ex}} = 2N^{\frac{-N}{2(N-1)}} (N-1)^{1/2} a_{\text{H,st}} , \quad (52)$$

while for even dimensions

$$j_{\text{ex}} = 2^{\frac{N-1}{2N-1}} N^{\frac{-N}{2N-1}} (2N-1)^{1/2} a_{\text{H,st}} . \quad (53)$$

Since  $j_{\text{ex}}$  and  $a_{\text{H,st}}$  are proportional, we obtain a relation between the scaled horizon velocity  $\bar{\Omega}_{\text{ex}}$  of the extremal rotating black holes and the scaled surface gravity  $\bar{\kappa}_{\text{st}}$  of the static black holes. For odd dimensions it reads

$$\bar{\kappa}_{\text{st}} = N^{\frac{N-2}{2(N-1)}} (N-1)^{1/2} \bar{\Omega}_{\text{ex}} , \quad (54)$$

and for even dimensions

$$\bar{\kappa}_{\text{st}} = 2^{\frac{-N}{2N-1}} N^{\frac{N-1}{2N-1}} (2N-1)^{1/2} \bar{\Omega}_{\text{ex}} . \quad (55)$$

Again, in five dimensions,  $\bar{\kappa}_{\text{st}}$  and  $\bar{\Omega}_{\text{ex}}$  coincide, while they are proportional in higher dimensions.

These KK relations hold also for vacuum black holes, obtained in the limit  $q \rightarrow 0$ .

## 4 Near-horizon solutions

The existence of extremal EMd and EM black hole solutions is supported by the existence of exact solutions, describing a rotating squashed  $AdS_2 \times S^{D-2}$  spacetime. These solutions correspond to the neighborhood of the event horizon of extremal black holes.

To obtain these exact near-horizon solutions for odd  $D$ -dimensions, we parametrize the metric as follows

$$\begin{aligned}
ds^2 = & v_1 \left( \frac{dr^2}{r^2} - r^2 dt^2 \right) + v_2 \sum_{i=1}^{N-1} \left( \prod_{j=0}^{i-1} \cos^2 \theta_j \right) d\theta_i^2 \\
& + v_2 v_3 \sum_{i=1}^N \left( \prod_{j=0}^{i-1} \cos^2 \theta_j \right) \sin^2 \theta_i (\varepsilon_i d\varphi_i - k r dt)^2 \\
& + v_2 (1 - v_3) \left\{ \sum_{i=1}^N \left( \prod_{j=0}^{i-1} \cos^2 \theta_j \right) \sin^2 \theta_i d\varphi_i^2 \right. \\
& \left. - \left[ \sum_{i=1}^N \left( \prod_{j=0}^{i-1} \cos^2 \theta_j \right) \sin^2 \theta_i \varepsilon_i d\varphi_i \right]^2 \right\} .
\end{aligned} \tag{56}$$

Here we have employed a new radial coordinate such that the horizon is located at  $r = 0$ . This position of the horizon can always be obtained by a transformation  $r \rightarrow r - r_H$ .

Moreover, we have shifted to a corrotating frame such that the angular velocity vanishes on the horizon. The corresponding parametrization for the gauge potential in the corrotating frame reads

$$A_\mu dx^\mu = (q_1 - q_2 k) r dt + q_2 \sum_{i=1}^N \left( \prod_{j=0}^{i-1} \cos^2 \theta_j \right) \sin^2 \theta_i \varepsilon_i d\varphi_i . \tag{57}$$

The dilaton field is simply given by  $\phi = u$ .

The parameters  $k$ ,  $v_i$ ,  $q_i$ , and  $u$  are constants, which satisfy a set of algebraic relations. In what follows we choose to determine them by using the near-horizon formalism proposed in [39, 40].

To that end let us denote by  $f(k, v_1, v_2, v_3, q_1, q_2, u)$  the Lagrangian density  $\sqrt{-g}\mathcal{L}$  evaluated for the near-horizon geometry Eq. (56) and potential Eq. (57) and integrated over the angular coordinates,

$$f(k, v_1, v_2, v_3, q_1, q_2, u) = \int d\theta_1 \dots d\theta_{N-1} d\varphi_1 \dots d\varphi_N \sqrt{-g} \mathcal{L} . \tag{58}$$

The field equations then follow from the variation of this functional. In particular, the derivative with respect to  $k$  and  $q_1$  yields the angular momenta and the charge,

$$\frac{\partial f}{\partial k} = 2J , \quad \frac{\partial f}{\partial q_1} = Q , \tag{59}$$

respectively, while the derivative with respect to the remaining parameters vanishes,

$$\frac{\partial f}{\partial v_i} = 0, \quad i = 1, 2, 3, \quad \frac{\partial f}{\partial q_2} = 0, \quad \frac{\partial f}{\partial u} = 0. \quad (60)$$

The entropy function is obtained by taking the Legendre transform of the above integral with respect to the parameter  $k$ , associated with all equal-magnitude angular momenta,  $J_1 = \dots = J_N = J$ , and with respect to the parameter  $q_1$ , associated with the charge  $Q$ ,

$$\mathcal{E}(J, k, Q, q_1, q_2, v_1, v_2, v_3, u) = 2\pi [NJk + Qq_1 - f(k, v_1, v_2, v_3, q_1, q_2, u)] . \quad (61)$$

Then the entropy associated with the black holes can be calculated by evaluating this function at the extremum,  $S = \mathcal{E}_{\text{extremum}}$ .

#### 4.1 Generic dilaton coupling

To obtain the near-horizon solutions, the set of equations Eqs. (59)-(60) must be solved. For a given spacetime dimension  $D = 2N + 1$ , the solutions can be expressed in terms of three independent parameters,  $v_1$ ,  $q_2$ , and  $u$ ,

$$\begin{aligned} v_2 &= 2(N-1)Nv_1, \\ v_3 &= N - \frac{2q_2^2 e^{-2hu}}{N(N-1)v_1}, \\ q_1 &= 0, \\ k &= \frac{1}{N\sqrt{N-1}}, \\ J &= \frac{2^{N+1}\sqrt{2N^2(N-1)v_1 - 4q_2^2 e^{-2hu}}}{N(N-1)^{3/2}(N-2)!v_1} (\pi N(N-1)v_1)^N, \\ Q &= -\frac{2^{N+2}\sqrt{2N^2(N-1)v_1 - 4q_2^2 e^{-2hu}}}{N(N-1)^{3/2}N!} (\pi N(N-1)v_1)^N \frac{q_2 e^{-2hu}}{v_1^2}. \end{aligned} \quad (62)$$

Interestingly,  $q_1$  vanishes and  $k$  is constant.

Let us now inspect the horizon charges obtained from this solution, Eq. (62). The horizon mass is given by

$$M_H = \frac{(D-1)(D-2)}{2(D-3)} \Omega J_H, \quad (63)$$

and the horizon angular momenta by

$$J_H = 2^N \sqrt{N-1} (N-2)! (N(N-1))^{N-3} \pi^N \left( 2N^2(N-1)v_1 - 4q_2^2 e^{-2hu} \right)^{3/2}. \quad (64)$$

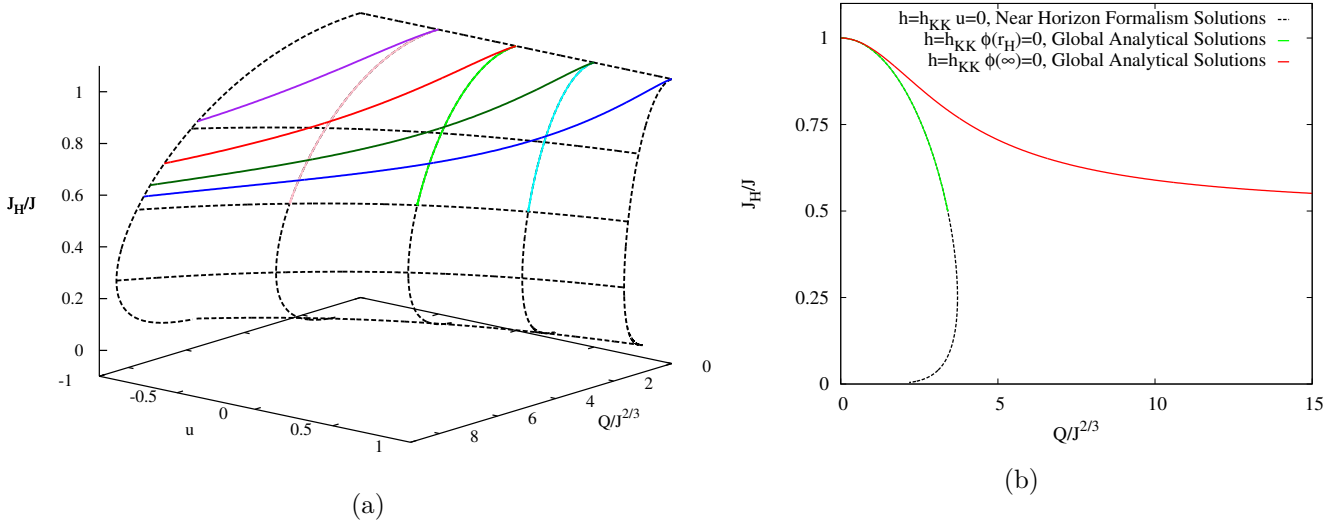


Figure 1: (a) Surface of near-horizon Emd solutions in five dimensions for dilaton coupling constant  $h = h_{KK}$ , scaled with the angular momentum: The horizon angular momenta  $J_H/J$  are shown versus the charge  $Q/J^{2/3}$  and the dilaton parameter  $u$ . The solid lines mark the global solutions. (b) Detail of (a) where the global solutions with  $\phi(\infty) = 0$  (red line) and with  $u = \phi(r_H) = 0$  (green line) are shown, together with the near-horizon Emd solutions with  $u = 0$  (black line).

The horizon area is obtained from the entropy function, Eq. (61)

$$A_H = \frac{\mathcal{E}}{4\pi} = \frac{J}{\sqrt{2(D-3)}}. \quad (65)$$

Thus relation Eq. (48) holds for generic values of the dilaton coupling constant  $h$  ( $h \neq 0$ ). Extremal dilatonic black holes thus show proportionality of their horizon area and their angular momenta.

The most intriguing feature of Eq. (62) is the presence of 3 free parameters. However, we know that these extremal black holes possess only 2 independent parameters (the electric charge  $Q$  and the angular momentum  $J$ , for instance). One would be tempted to state that the existence of an extra independent parameter in the near-horizon Emd solutions is related to the existence of non-globally realized near-horizon Emd solutions. Although these non-globally realized solutions are really present among the near-horizon Emd solutions, as we will show below, the question is more subtle. The key point here is the invariance under a scale transformation associated with the dilaton

$$\begin{aligned} \tilde{x}^\mu &= \lambda^{-1} x^\mu, \\ \tilde{\phi} &= \phi + \frac{1}{h} \log \lambda, \end{aligned}$$

$$\tilde{F}_{\mu\nu} = \lambda^2 F_{\mu\nu} . \quad (66)$$

Note that under this transformation the value of the dilaton at the horizon may be set to any given value, so the parameter  $u$  may be eliminated by such a transformation (i.e., one can set  $u = 0$  without loss of generality). We illustrate this fact in Figs. 1. In Fig. 1(a) we plot the scaled horizon angular momenta  $J_H/J$  as a function of  $u$  and  $Q/J^{2/3}$ , for the dilaton coupling constant  $h = h_{KK}$  in five dimensions. On the surface we show black dashed curves corresponding to cuts with constant  $u$  and cuts with constant  $J_H/J$ . We also exhibit with solid lines sets of globally realized extremal solutions. The curves in light blue, light green, and pink are solutions with constant  $u = \phi(r_H)$ , and the curves in dark blue, dark green, red, and purple are solutions with constant  $\phi(\infty)$ . All these globally realized curves range from  $J_H/J = 1$  to  $J_H/J = 1/2$  (this last limit depending on  $h$ ; its lowest value is  $1/4$  for EM  $h = 0$ ). The curves with constant  $u = \phi(r_H)$  have finite length while those with constant  $\phi(\infty)$  have infinite length. However, all of them are equivalent to each other. The curves with constant  $u = \phi(r_H)$  transform into each other under a transformation of the type Eq. (66) with a constant  $\lambda$ ; the same holds among curves with constant  $\phi(\infty)$ . A transformation among the curves with constant  $u = \phi_H$  and the curves with constant  $\phi(\infty)$  requires a factor  $\lambda$  that varies with  $Q$ . Since  $J_H/J$  is invariant under Eq. (66), the requirement for two points on the surface to be equivalent is that they have the same  $J_H/J$  value. Note that  $Q/J^{2/3}$  is not invariant but transforms as  $\tilde{Q}/\tilde{J}^{2/3} = \lambda Q/J^{2/3}$ . That means if one changes the  $Q/J^{2/3}$  axis to  $e^{h\phi(\infty)}Q/J^{2/3}$ , all the color curves collapse into the red curve. In fact, the whole upper part of the surface with  $J_H/J \geq 1/2$  collapses into the red curve.

Going back to the point of the existence of non-globally realized near-horizon EMD solutions, we see that solutions with  $J_H/J \leq 1/2$  do not exist globally for  $h = h_{KK}$ . We demonstrate this in Fig. 1(b). There only the globally realized solutions with  $\phi(\infty) = 0$  and  $\phi(r_H) = 0$  are included, together with the near-horizon solutions with  $u = 0$ . Near-horizon EMD solutions (in black) with  $J_H/J < 1/2$  are not realized globally. (They correspond to the region where the black and the green curves do not overlap.)

## 4.2 Kaluza-Klein case

Since the black hole for the Kaluza-Klein value of the dilaton coupling is explicitly known, we can obtain the near-horizon limit of the analytic solution.

We change the metric Eq. (42) to a corrotating frame, shift the radial coordinate to be centered on the horizon, and make the near-horizon limit together with an appropriate gauge transformation on the gauge potential Eq. (45). The resulting metric can be written in a similar form as in Eq. (56). The gauge vector can also be written in the same form as in Eq. (57). The dilaton Eq. (46) is given by a parameter  $\phi = u$  in the near-horizon limit. All these parameters satisfy the following relations with the

parameters  $a$  and  $\alpha$  from the Kaluza-Klein solution:

$$\begin{aligned}
v_1 &= \frac{1}{2} a^2 \frac{(1 + N \cosh(\alpha)^2 - N)^{\frac{1}{D-2}}}{(N-1)^2} , \\
v_2 &= 2N(N-1)v_1 , \\
v_3 &= \frac{N \cosh(\alpha)^2}{1 - N + N \cosh(\alpha)^2} , \\
k &= \frac{1}{N\sqrt{N-1}} , \\
q_1 &= 0 , \\
q_2 &= -\frac{Na \sinh(\alpha)}{1 + N \cosh(\alpha)^2 - N} .
\end{aligned} \tag{67}$$

Note that these relations are compatible with the near-horizon geometry for generic dilaton coupling Eq. (62), in the particular case of  $h = h_{KK}$ .

In this case, since we derive the near-horizon limit of the global solution, we also obtain a relation for the dilaton parameter,

$$u = -\frac{\sqrt{2(D-1)}}{2\sqrt{D-2}} \ln(1 + N \cosh(\alpha)^2 - N) . \tag{68}$$

We note, that this relation was not found by employing the near-horizon formalism in the previous section 4.1. Here this relation is only found as a result of explicitly knowing the global solution and the fact that the dilaton is required to vanish at infinity. So this solution corresponds to the red curve in Figs. 1.

### 4.3 Einstein-Maxwell case

Surprisingly, the EM case is rather different from the EMd case. In particular, there is not only one set of solutions, as in the EMd case, but there are two sets of solutions, which we label currently as the first branch and the second branch of solutions. The five-dimensional case was discussed before [19, 41]. Moreover, the EM solutions depend only on two parameters, since there is no dilaton parameter.

For a given spacetime dimension  $D = 2N + 1$ , the first set of solutions can be expressed in terms of the independent parameters  $v_1$  and  $q_2$ . Thus the first branch is given by

$$\begin{aligned}
v_2 &= 2(N-1)Nv_1 , \\
v_3 &= N - \frac{2q_2^2}{N(N-1)v_1} , \\
q_1 &= 0 , \\
k &= \frac{1}{N\sqrt{N-1}} ,
\end{aligned}$$

$$\begin{aligned}
J &= \frac{2^{N+1} \sqrt{2N^2(N-1)v_1 - 4q_2^2}}{N(N-1)^{3/2}(N-2)!v_1} (\pi N(N-1)v_1)^N, \\
Q &= -\frac{2^{N+2} \sqrt{2N^2(N-1)v_1 - 4q_2^2}}{N(N-1)^{3/2}N!} (\pi N(N-1)v_1)^N \frac{q_2}{v_1^2}.
\end{aligned} \tag{69}$$

As in the EMd case, in this EM solution  $q_1$  vanishes and  $k$  is constant. Moreover, by defining  $\bar{q}_2 = q_2 e^{-hu}$  and  $\bar{Q} = Q e^{hu}$  in the EMd solution Eq. (62), this first EM branch is obtained. Because  $e^{-2hu}$  is multiplying  $q_2$  everywhere, we re-obtain the MP solution, when setting  $q_2 = 0$ .

Inspecting the horizon charges obtained from this solution Eq. (69), we find the horizon mass

$$M_H = \frac{(D-1)(D-2)}{2(D-3)} \Omega J_H, \tag{70}$$

and the horizon angular momenta

$$J_H = 2^N \sqrt{N-1} (N-2)! (N(N-1))^{N-3} \pi^N (2N^2(N-1)v_1 - 4q_2^2)^{3/2}. \tag{71}$$

The horizon area is obtained from the entropy function, Eq. (61)

$$A_H = \frac{\mathcal{E}}{4\pi} = \frac{J}{\sqrt{2(D-3)}}. \tag{72}$$

Clearly, relation Eq. (48) holds along this first branch, expressing proportionality of the horizon area and the angular momenta.

The near-horizon equations, however, allow for a second set of solutions, which can be expressed in terms of the independent parameters  $v_1$  and  $v_2$ . These solutions form the second branch and are given by

$$\begin{aligned}
v_3 &= \frac{v_2}{4(N-1)(N-2)v_1} - \frac{1}{N-2}, \\
k &= \frac{2\sqrt{N-1}v_1}{v_2\sqrt{v_2 + 4(1-N)v_1}} \sqrt{4(N-1)^2v_1 - v_2}, \\
q_1 &= \frac{\sqrt{2N-1}}{\sqrt{N-2}} \sqrt{\frac{v_1}{v_2} \frac{2N(N-1)v_1 - v_2}{v_2 + 4(1-N)v_1}}, \\
q_2 &= \frac{\sqrt{2N-1}}{4\sqrt{N-2}(N-1)} \sqrt{\frac{v_2}{v_1} \sqrt{4(N-1)^3v_1 + (1-N)v_2}}, \\
J &= \frac{(\pi v_2)^N}{(N-1)!} \frac{v_2 - 4(N-1)v_1}{(N-1)^{3/2}(N-2)^{3/2}v_1^{3/2}\sqrt{v_2}} \sqrt{(N-1)(4(N-1)^2v_1 - v_2)}, \\
Q &= \frac{-2(\pi v_2)^N}{(N-1)!} \frac{\sqrt{2N-1}}{\sqrt{N-1}(N-2)} \frac{4(N-1)v_1 - v_2}{v_1 v_2}.
\end{aligned} \tag{73}$$



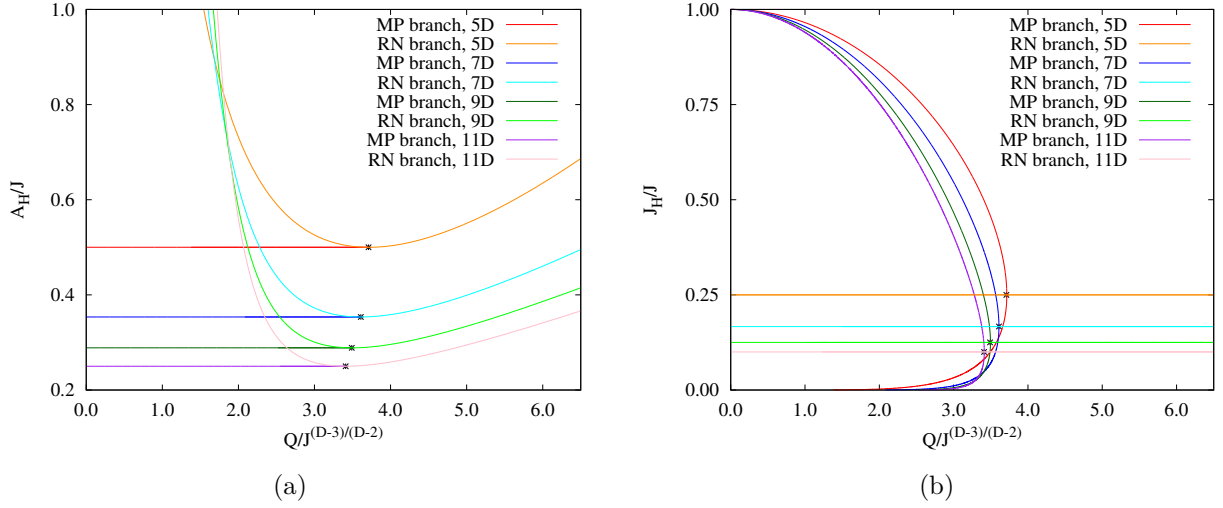


Figure 2: Near-horizon EM solutions in several dimensions: The horizon area  $A_H$  (a) and the horizon angular momenta  $J_H$  (b) are shown versus the charge  $Q$  (quantities are scaled by the angular momenta  $J$ .) The asterisks mark the matching points of the two branches. The first branch is realized globally from the MP solution to the matching point, while the second branch is realized globally from the matching point to the RN solution.

The horizon charges of the solutions on the second branch are given by

$$M_H = \frac{(D-1)(D-2)}{2(D-3)} \Omega J_H, \quad (74)$$

$$J_H = \frac{J}{D-1}, \quad (75)$$

and the horizon area is again obtained from the entropy function, Eq. (61)

$$A_H = \frac{\mathcal{E}}{4\pi} = \frac{(\pi v_2)^N \sqrt{v_2 - 4(N-1)v_1}}{\sqrt{N-2} \sqrt{N-1} (N-1)! \sqrt{v_1 v_2}}. \quad (76)$$

For this branch of solutions the horizon area is not proportional to the angular momenta. Instead, the horizon angular momenta are proportional to the total angular momenta [19].

Figs. 2 exhibit the two branches of solutions for near-horizon solutions in odd dimensions, from five to eleven. In particular, we show the horizon area  $A_H$  (a) and the horizon angular momenta  $J_H$  (b) versus the charge  $Q$ , scaled by the angular momenta  $J$ . The first branch, starting from the MP solution, extends only up to a maximal value of the charge  $Q$ , for given angular momenta  $J$ . At this critical value it does not end, however, but it continues backwards to smaller charges.

The second branch, on the other hand, extends over the full axis. It smoothly reaches the extremal static RN solution, when  $J \rightarrow 0$ , but it also extends all the way

to vanishing electric charge  $Q$ . Most importantly, however, this second branch crosses the first branch precisely at its critical point. Here all physical quantities match for the two branches. This matching point is indicated in the figures by an asterisk. It is this matching point, which also delimits the globally realized parts of these branches of solutions. The first branch is realized globally from the MP solution to the matching point, while the second branch is realized globally from the matching point to the RN solution.

Thus for extremal EM black holes in higher odd dimensions the branch structure is analogous to the five-dimensional case [19, 41]. In the following we will denote the branches as the MP branch and the RN branch, since they start at the extremal MP solution and the extremal RN solution, respectively.

## 5 Numerical solutions

After a short discussion of the numerical procedure and the boundary conditions, we present our results for black holes in 5, 7, and 9 dimensions. We discuss the domains of existence, the global properties, in particular, the gyromagnetic ratio, and the horizon properties, where the surface gravity  $\kappa$  and the horizon angular velocity  $\Omega$  are associated with a critical behavior.

This critical behavior was observed before for static EMd black holes [36]. Here, at the critical value of the dilaton coupling  $h_{\text{cr}}$ ,

$$h_{\text{cr}} = \frac{D-3}{\sqrt{2(D-2)}} , \quad (77)$$

the surface gravity  $\kappa$  remains finite in the extremal limit. In contrast,  $\kappa$  diverges for  $h > h_{\text{cr}}$ , while  $\kappa \rightarrow 0$  for  $h < h_{\text{cr}}$  in the extremal limit. Comparing this critical value  $h_{\text{cr}}$  to the KK value  $h_{\text{KK}}$ , we note, that

$$\begin{aligned} h_{\text{cr}} &= h_{\text{KK}} \text{ for } D = 5 , \\ h_{\text{cr}} &> h_{\text{KK}} \text{ for } D > 5 . \end{aligned} \quad (78)$$

Since the solutions have a scaling symmetry Eq. (26), we typically exhibit scaled physical quantities, where we scale with respect to appropriate powers of the mass  $M$ . In particular, we employ the charge to mass ratio  $q$  to demonstrate the dependence on the charge.

The domain of existence of these black holes increases with increasing dilaton coupling constant  $h$ , since the maximal value of the scaled charge  $q$  increases with  $h$  according to

$$q_{\text{max}} = \sqrt{\frac{D-3}{2(D-2)}} + h^2 , \quad (79)$$

i.e., for the Kaluza-Klein coupling constant  $h_{\text{KK}}$  the maximal value of the scaled charge is given by  $q_{\text{max}} = 1$ , independent of the dimension  $D$ .

The gyromagnetic ratio  $g$  of higher dimensional black holes has drawn much interest, ever since perturbations in the charge in the EM case ( $h = 0$ ) yielded for MP black holes the intriguing lowest order result [10]

$$g_{\delta q} = D - 2 + o(q^2) . \quad (80)$$

The same result was obtained when considering first order perturbations in the angular momentum for the charged static solutions in the EM case ( $h = 0$ ) [14]

$$g_{\delta j} = D - 2 + o(j^2) . \quad (81)$$

Nevertheless, this result was shown not to hold in general for higher order perturbations in the charge [13, 15, 16], and non-perturbatively for arbitrary values of  $Q$  and  $J$  [17, 18]. However, it still represents an important limiting value for EM and EMd black holes, attained for small values of the charge to mass ratio  $q$ . In fact, in the EMd case ( $h \neq 0$ ) first order perturbations in the angular momentum for the charged static solutions yield, in our conventions in terms of  $q = Q/M$  and a generic dilaton coupling  $h$ , the expression [14]

$$g_{\delta j} = \frac{(D-1)(D-2)(D-3)[D-3+X]}{4h^2(D-2)^2q^2 + (D-1)(D-3)[D-3+X]} , \quad (82)$$

where

$$X^2 = 2(D-2)[2h^2(D-2) + 3 - D]q^2 + (D-3)^2 . \quad (83)$$

## 5.1 Numerical procedure and boundary conditions

In order to solve the coupled system of ODE's, we take advantage of the existence of a first integral of that system,

$$\frac{r^{D-2}m^{(D-5)/2}}{f^{(D-3)/2}} \sqrt{\frac{mn}{f}} \left( \frac{da_0}{dr} + \frac{\omega}{r} \frac{da_\varphi}{dr} \right) = -\frac{e^{2h\phi}}{A(S^{D-2})} Q , \quad (84)$$

to eliminate  $a_0$  from the equations, leaving a system of one first order equation (for  $n$ ) and four second order equations.

For the numerical calculations we take units such that  $16\pi G_D = 1$ . We introduce a compactified radial coordinate. For the non-extremal solutions we take the compactified coordinate to be  $\bar{r} = 1 - r_H/r$ . In the extremal case we employ  $\bar{r} = \frac{r}{1+r}$  [42]. (Note, that we are using an isotropic coordinate  $r$ , so  $r_H = 0$  in the extremal case.) We employ a collocation method for boundary-value ordinary differential equations, equipped with an adaptive mesh selection procedure [43]. Typical mesh sizes include  $10^3 - 10^4$  points. The solutions have a relative accuracy of  $10^{-10}$ . The estimates of the relative errors of the global charges and the magnetic moment are of order  $10^{-6}$ , giving rise to an estimate of the relative error of  $g$  of order  $10^{-5}$ .

To obtain asymptotically flat solutions the metric functions should satisfy the boundary conditions

$$f|_{r=\infty} = m|_{r=\infty} = n|_{r=\infty} = 1, \quad \omega|_{r=\infty} = 0. \quad (85)$$

For the gauge potential we choose a gauge, in which it vanishes at infinity

$$a_0|_{r=\infty} = a_\varphi|_{r=\infty} = 0. \quad (86)$$

For the dilaton field we choose

$$\phi|_{r=\infty} = 0. \quad (87)$$

Note, that any finite value of the dilaton field at infinity can always be transformed to zero via  $\phi \rightarrow \phi - \phi(\infty)$ ,  $r \rightarrow r e^{h\phi(\infty)}$ ,  $a_0 \rightarrow a_0 e^{-h\phi(\infty)}$ .

Requiring the horizon to be regular, the metric functions must satisfy the boundary conditions

$$f|_{r=r_H} = m|_{r=r_H} = n|_{r=r_H} = 0, \quad \omega|_{r=r_H} = r_H \Omega, \quad (88)$$

where  $\Omega$  is the horizon angular velocity, defined in terms of the Killing vector  $\chi$ , Eq. (15).

The gauge potential satisfies at the horizon the conditions

$$\chi^\mu A_\mu|_{r=r_H} = \Phi_H = (a_0 + \Omega a_\varphi)|_{r=r_H}, \quad \left. \frac{da_\varphi}{dr} \right|_{r=r_H} = 0, \quad (89)$$

with the constant horizon electrostatic potential  $\Phi_H$ . The boundary condition for the dilaton field reads

$$\left. \frac{d\phi}{dr} \right|_{r=r_H} = 0. \quad (90)$$

Since the KK solutions are known analytically, we can use them as a test for the accuracy of the numerical calculations, by choosing the dilaton coupling constant  $h = h_{\text{KK}}$ . Other general tests are provided by the Smarr formula Eq. (22) and the relation Eq. (23).

## 5.2 Expansions

The asymptotic expansion of the metric, the gauge potential, and the dilaton field reads

$$\begin{aligned} f &= 1 - \frac{M}{(D-2)A(S^{D-2})} \frac{1}{r^{D-3}} + \dots, \\ m &= 1 - \frac{(D-4)M}{(D-2)(D-3)A(S^{D-2})} \frac{1}{r^{D-3}} + \dots, \\ n &= 1 - \frac{(D-4)M}{(D-2)(D-3)A(S^{D-2})} \frac{1}{r^{D-3}} + \dots, \\ \omega &= \frac{J}{2A(S^{D-2})} \frac{1}{r^{D-2}} + \dots, \end{aligned}$$

$$\begin{aligned}
a_0 &= \frac{Q}{(D-3)A(S^{D-2})} \frac{1}{r^{D-3}} + \dots , \\
a_\varphi &= -\frac{\mu_{\text{mag}}}{(D-3)A(S^{D-2})} \frac{1}{r^{D-3}} + \dots , \\
\phi &= \frac{\Sigma}{(D-3)A(S^{D-2})} \frac{1}{r^{D-3}} + \dots .
\end{aligned} \tag{91}$$

The global mass  $M$ , the global angular momenta  $J$ , the electric charge  $Q$ , the dilaton charge  $\Sigma$ , and the magnetic moment  $\mu_{\text{mag}}$ , can be read off from this expansion. Note that in the non-extremal case, only three of these parameters are free. In the extremal case there are only two free parameters.

For the expansion at the horizon we should distinguish explicitly whether the solutions are non-extremal or extremal. In the non-extremal case the expansion of the functions at the horizon reads

$$\begin{aligned}
f &= f_2 \delta^2 (1 - \delta) + O(\delta^4) , \\
m &= m_2 \delta^2 (1 - 3\delta) + O(\delta^4) , \\
n &= n_2 \delta^2 (1 - 3\delta) + O(\delta^4) , \\
\omega &= r_H \Omega (1 + \delta) + O(\delta^2) , \\
a_0 &= a_{0,0} + O(\delta^2) , \\
a_\varphi &= a_{\varphi,0} + O(\delta^2) , \\
\phi &= \phi_0 + O(\delta^2) ,
\end{aligned} \tag{92}$$

where  $\delta = r/r_H - 1$  and  $f_2, m_2, n_2, a_{0,0}, a_{\varphi,0}$ , and  $\phi_0$  are constant.

In the extremal case the situation is very different. The expansion near the horizon  $r_H = 0$  is

$$\begin{aligned}
f &= f_4 r^4 + f_\alpha r^\alpha + o(r^6) , \\
m &= m_2 r^2 + m_\beta r^\beta + o(r^4) , \\
n &= n_2 r^2 + n_\gamma r^\gamma + o(r^4) , \\
\omega &= \omega_1 r + \omega_2 r^2 + o(r^3) , \\
a_0 &= a_{0,0} + a_{0,\lambda} r^\lambda + o(r^2) , \\
a_\phi &= a_{\phi,0} + a_{\phi,\mu} r^\mu + o(r^2) , \\
\phi &= \phi_0 + \phi_\nu r^\nu + o(r^2) .
\end{aligned} \tag{93}$$

It is interesting to note, that, in general, the exponents  $\alpha, \beta, \gamma, \lambda, \mu$ , and  $\nu$  are non-integer. Note, that  $\omega$  is the only function with the usual expansion at the horizon. For the other functions, the next to leading order is given by a term with a non-integer exponent. The ranges are

$$\begin{aligned}
4 < \alpha < 6 , \quad 2 < \beta < 4 , \quad 2 < \gamma < 4 , \\
0 < \lambda < 2 , \quad 0 < \mu < 2 , \quad 0 < \nu < 2 .
\end{aligned} \tag{94}$$

In the pure Einstein-Maxwell case ( $h = 0$ ) the expansion contains similarly non-integer exponents (but there is no dilaton function). This feature is found in both EM branches (i.e., in the MP branch and in the RN branch).

For the numerical integration the following reparametrization of the functions was made,

$$\begin{aligned} f &= \hat{f}x^2, & m &= \hat{m}, & n &= \hat{n}, \\ \omega &= \hat{\omega}(1-x)^2, & a_k &= \hat{a}_k/x^2, & \phi &= \hat{\phi}/x^2. \end{aligned} \quad (95)$$

Note, that all the redefined functions except for  $\hat{\omega}$  now start with an  $x^2$ -term in the compactified coordinate  $x = r/(r+1)$ . (The reparametrization of  $\omega$  is not related to the expansion at the horizon. It is done in order to be able to fix the angular momentum by a boundary condition). Numerically this reparametrization is used to deal with the possible divergence of the first- and second-order derivatives of any field functions.

### 5.3 $D = 5$

Here we present our numerical results for black holes with equal magnitude angular momenta in 5 dimensions. We begin with a discussion of the solutions for a generic value of the dilaton coupling constant,  $h = 2$ . Then we discuss the dependence of the solutions on the dilaton coupling constant,  $0 \leq h < \infty$ , including the Einstein-Maxwell case ( $h = 0$ ) and the Kaluza-Klein case ( $h = h_{\text{KK}} = \sqrt{2/3}$ ). The formulae for the latter are collected in Section 3. We note, that uniqueness of the stationary black holes in 5D Einstein-Maxwell and Einstein-Maxwell-dilaton gravity were discussed by Yazadjiev [44].

#### 5.3.1 Dilaton coupling constant $h = 2$

Let us first address the domain of existence of rotating EMd black holes with equal-magnitude angular momenta. For such black holes the domain of existence is always bounded. The boundary is provided by the set of extremal solutions. However, when we consider quantities, that do not depend on the direction of the rotation, the set of static solutions provides a part of the boundary. The non-extremal rotating solutions then reside within this boundary, while solutions outside this boundary exhibit naked singularities.

We illustrate the domain of existence of EMd black holes with dilaton coupling constant  $h = 2$  for the scaled horizon area  $a_{\text{H}} = A_{\text{H}}/M^{3/2}$  in Fig. 3(a). Considering  $a_{\text{H}}$  versus the scaled charge  $q$ , the extremal and static solutions form the lower and upper boundaries of the domain of existence, respectively. In the extremal limit, the horizon area of the static black holes vanishes, while the rotating extremal black holes have finite horizon area. Thus only static extremal black holes have vanishing area, while all other black holes have finite area.

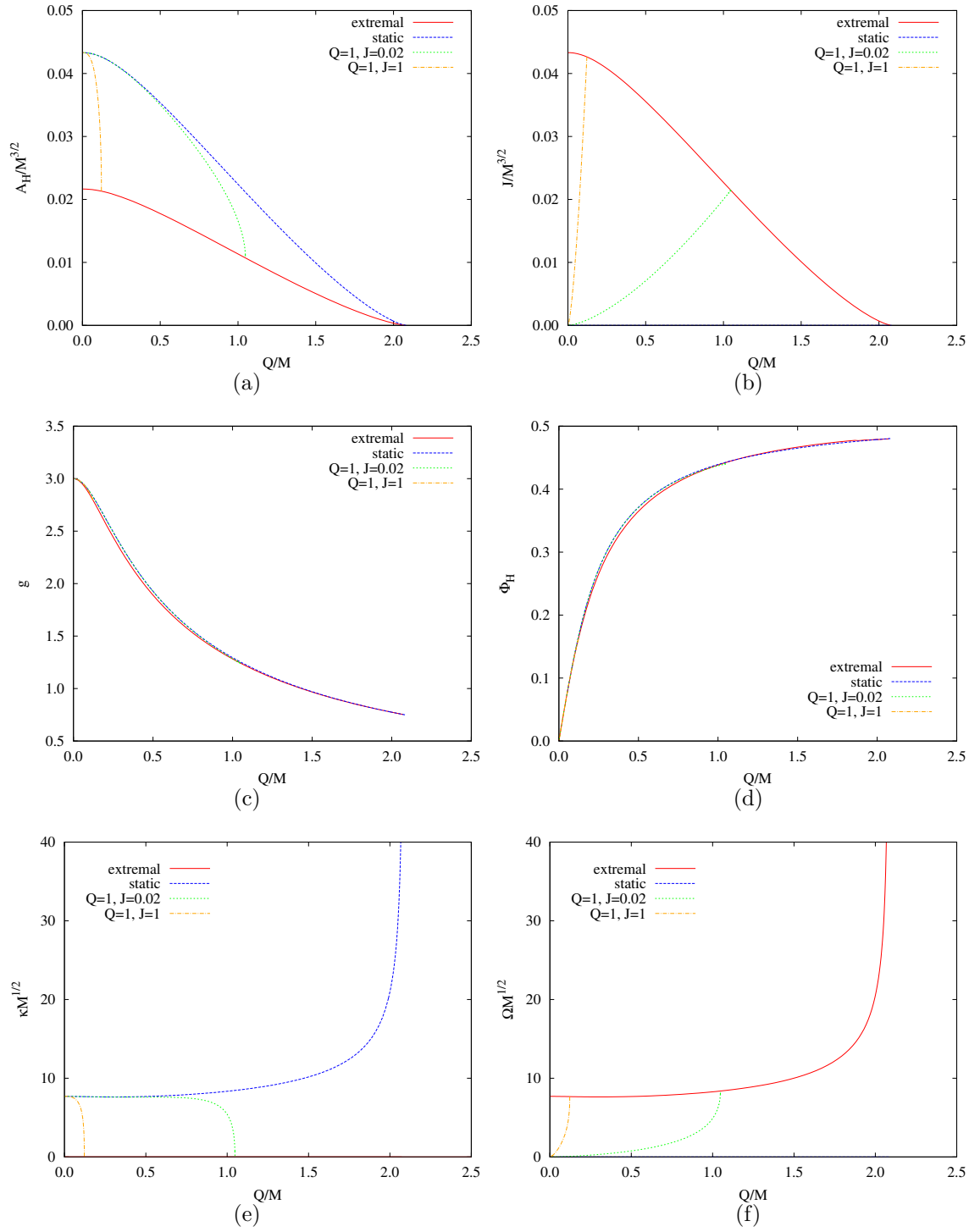


Figure 3: Properties of EMD black hole solutions in five dimensions for dilaton coupling constant  $h = 2$ . (a) The scaled area  $a_H = A_H/M^{3/2}$  versus the scaled charge  $q = |Q|/M$  for extremal and for static solutions, providing the boundary of the domain of existence. Also shown is  $a_H$  versus  $q$  for two further sets of non-extremal solutions ( $Q = 1, J = 0.02$  and  $Q = 1, J = 1$ ). For the same sets of (extremal and non-extremal) solutions we exhibit in (b) the scaled angular momenta  $j = J/M^{3/2}$  versus  $q$ , (c) the gyromagnetic ratio  $g$  versus  $q$ , (d) the horizon electrostatic potential  $\Phi_H$  versus  $q$ , (e) the scaled surface gravity  $\bar{\kappa} = \kappa M^{1/2}$  versus  $q$ , (f) the scaled horizon angular velocity  $\bar{\Omega} = \Omega M^{1/2}$  versus  $q$ .

We also exhibit in Fig. 3(a) two further sets of solutions, which are non-extremal, except at their respective endpoints. Here the charge  $Q$  and the angular momenta  $J$  are kept fixed, in particular, the choices are  $Q = 1, J = 0.02$  and  $Q = 1, J = 1$ , while the (isotropic) horizon radius  $r_H$  is varied. These two sets start at a small value of  $q$  and end at the respective extremal solutions.

Next to the area we illustrate the scaled angular momenta  $j = J/M^{3/2}$  versus  $q$  in Fig. 3(b). We note the proportionality of the scaled angular momenta  $j$  and the area  $a_H$ , Eq. (48), for the extremal solutions. Since we have chosen  $J \geq 0$ , the non-extremal rotating solutions reside within the boundary formed by the extremal and the static solutions, which have  $j = 0$ .

Fig. 3(c) exhibits the gyromagnetic ratio  $g$  of these black holes. For small charge, the perturbative value  $g_{\delta q} = 3$  is found [10], while for larger values of the charge considerable deviations from this value arise, as shown in higher order perturbation theory [13, 15, 16]. The curves formed by the gyromagnetic ratio  $g$  of the extremal black holes and by the gyromagnetic ratio  $g_{\delta j}$ , Eq. (82), obtained for black holes in the static limit  $J \rightarrow 0$  [14], enclose the domain, where the gyromagnetic ratio can take its values. Since the extremal and the ‘static’ curve are very close to each other, the ‘static’ values represent a good approximation for a given value of  $q$ . Consequently, the gyromagnetic ratio is not well resolved for the non-extremal sets of solutions in the figure. We recall, that in the KK case,  $g$  is given by a single curve, i.e., the KK domain of  $g$  is only one-dimensional.

The situation is similar for the horizon electrostatic potential  $\Phi_H$ , which we exhibit in Fig. 3(d). Again the static and the extremal solutions forming the boundaries for the admissible values of this quantity are very close to each other, thus the values of the non-extremal black holes are not well discernable here, either. In the KK case  $\Phi_H$  is again given by a single curve, i.e., its KK domain is only one-dimensional.

The surface gravity  $\kappa$  of these black holes is addressed in Fig. 3(e), where the scaled surface gravity  $\bar{\kappa} = \kappa M^{1/2}$  is exhibited versus the scaled charge  $q$ . The static set of solutions here forms the upper boundary, while the set of extremal solutions, having  $\kappa = 0$  (for finite  $J$ ), forms the lower boundary. At the static extremal black hole, the static curve diverges,  $\kappa = \infty$  [36, 45], since  $h > h_{\text{cr}} = \sqrt{2/3}$ , Eq. (77). Thus for the set of extremal black holes the surface gravity jumps from zero, its value for finite angular momentum, to infinity in the static limit.

Finally, we exhibit the scaled horizon angular velocity  $\bar{\Omega} = \Omega M^{1/2}$  in Fig. 3(f). Here the static black holes, possessing  $\Omega = 0$ , form the lower boundary, while the extremal black holes form the upper boundary, with all other black holes assuming values in-between. Thus the scaled horizon angular velocity and the surface gravity show an analogous behavior, where the static and extremal solutions, however, have switched roles.



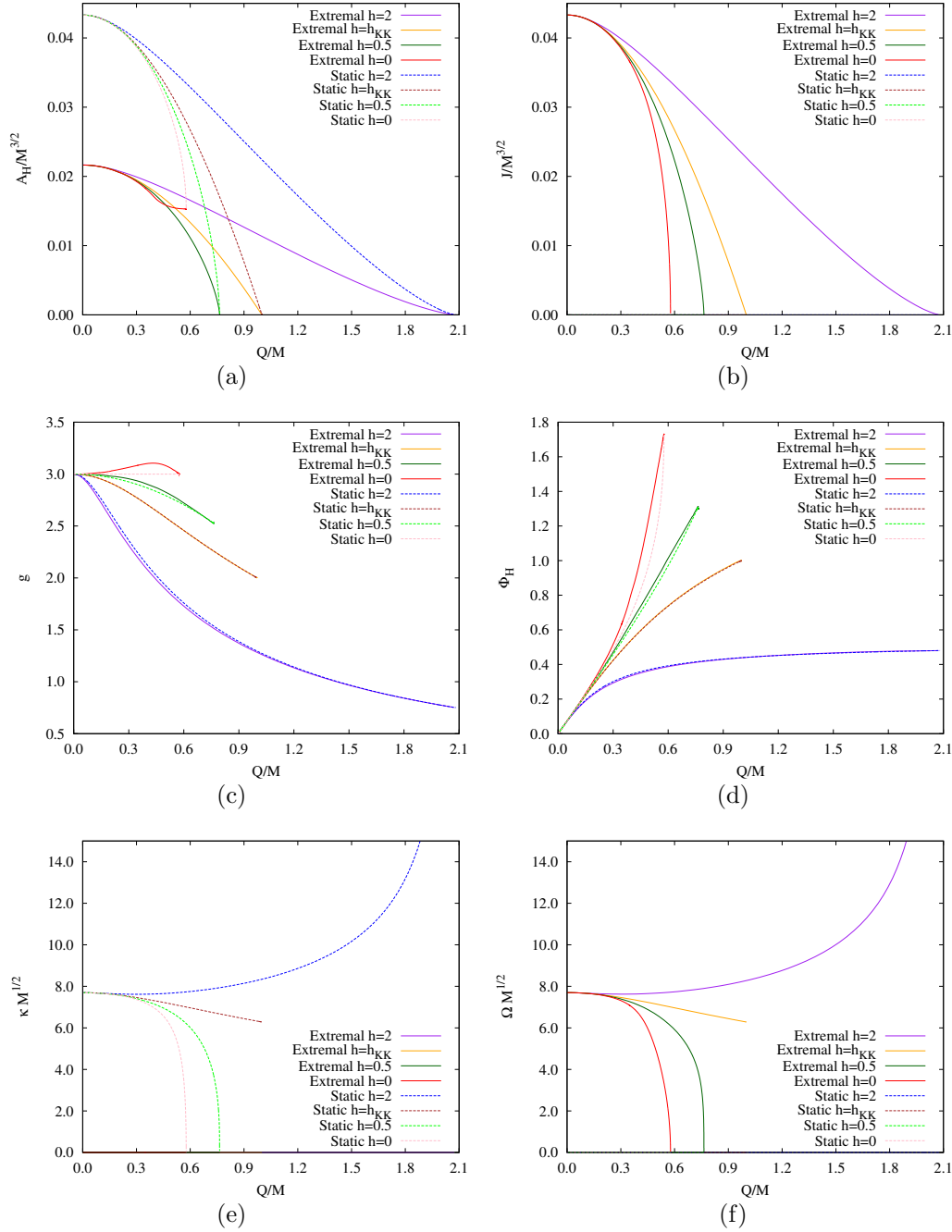


Figure 4: Properties of EMd black hole solutions in five dimensions are shown for several values of the dilaton coupling constant  $h$ :  $h = 0$  (EM),  $0.5$ ,  $\sqrt{2/3}$  (KK),  $2$ . (a) The scaled area  $a_H = A_H/M^{3/2}$  versus the scaled charge  $q = |Q|/M$  for extremal and for static solutions, providing the boundary of the domain of existence. For the same sets of (extremal and non-extremal) solutions we exhibit in (b) the scaled angular momenta  $j = J/M^{3/2}$  versus  $q$ , (c) the gyromagnetic ratio  $g$  versus  $q$ , (d) the horizon electrostatic potential  $\Phi_H$  versus  $q$  (e) the scaled surface gravity  $\bar{\kappa} = \kappa M^{1/2}$  versus  $q$ , (f) the scaled horizon angular velocity  $\bar{\Omega} = \Omega M^{1/2}$  versus  $q$ .

### 5.3.2 $h$ -dependence

To study the dependence of these black holes on the dilaton coupling constant  $h$ , we now consider several fixed values of  $h$ :  $h = 0$ , corresponding to the EM case,  $h = 0.5$ ,  $h = \sqrt{2/3}$ , corresponding to the KK case, and  $h = 2$ , the case studied above in more detail. We exhibit properties of these solutions in Figs. 4. In particular, we show the extremal and the static solutions, which form the boundary of the domain of existence for these black holes. All non-extremal rotating black holes are located inside this boundary. The quantities shown are the scaled horizon area  $a_H$  (Fig. 4(a)), the scaled angular momenta  $j$  (Fig. 4(b)), the gyromagnetic ratio  $g$  (Fig. 4(c)), the horizon electrostatic potential  $\Phi_H$  (Fig. 4(d)), the scaled surface gravity  $\bar{\kappa}$  (Fig. 4(e)), and the scaled horizon angular velocity  $\bar{\Omega}$  (Fig. 4(f)).

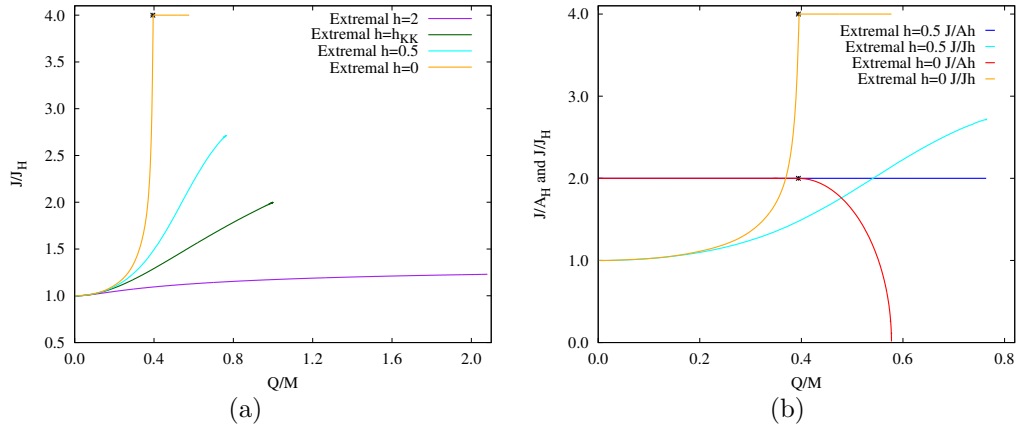


Figure 5: (a)  $J/J_H$  is shown versus the scaled charge  $q$  for extremal EMD black hole solutions in five dimensions for  $h = 0$  (EM),  $0.5$ ,  $\sqrt{2/3}$  (KK), and  $2$ . (b) The ratios  $J/A_H$  and  $J/J_H$  versus  $q$  for  $h = 0$  and  $h = 0.5$ . The asterisks mark the matching point of the two EM branches.

For the area and the angular momenta, we note again the proportionality for finite dilaton coupling. For the EM case,  $h = 0$ , this proportionality holds only along the MP branch, while it is violated on the RN branch of the solutions. We demonstrate this further in Figs. 5, where we exhibit the branch structure for these solutions. In particular, we show the ratio  $J/J_H$  versus the scaled charge  $q$  in Fig. 5(a) for the above set of coupling constants and the ratios  $J/A_H$  and  $J/J_H$  versus  $q$  for  $h = 0$  and  $h = 0.5$  in Fig. 5(b).

The figures clearly reveal the two-branch structure of the extremal EM solutions, together with their matching point, and the single-branch structure of the EMD solutions. Comparison with Figs. 2 shows, that for the EM solutions only the first part of the near-horizon MP branch and the second part of the near-horizon RN branch are realized globally. For the EMD solutions, on the other hand, the surfaces of near-horizon

solutions are reduced to single curves, that are - in part - realized globally, for arbitrary finite value of the dilaton coupling  $h$  (compare Figs. 1).

In the extremal limit, the horizon area of the static black holes vanishes as long as the dilaton coupling constant  $h$  is non-vanishing, no matter how small it is. In contrast, for the static EM black holes the area remains finite. The EM limit,  $h \rightarrow 0$ , of the extremal static black hole is therefore not smoothly approached.

Turning to the gyromagnetic ratio  $g$ , exhibited in Fig. 4(c), we note, that it attains the perturbative value  $g_{\delta q} = 3$  [10] for small  $q$ , independent of the dilaton coupling constant  $h$ . For a fixed value of  $h$ , the curves formed by the gyromagnetic ratio  $g$  of the extremal black holes and by the gyromagnetic ratio  $g_{\delta j}$ , Eq. (82), obtained for black holes in the static limit  $J \rightarrow 0$  [14], enclose the domain, where the gyromagnetic ratio can take its values.

In the EM case, the perturbative value obtained for small  $q$ ,  $g_{\delta q} = 3$ , coincides with the perturbative value for small  $j$ ,  $g_{\delta j} = 3$ , which forms a horizontal line. At the same time, this ‘static’ limit constitutes a lower bound for the gyromagnetic ratio of all EM black holes with equal magnitude angular momenta [13, 17, 18].

For small but finite values of the dilaton coupling constant  $h$ , the gyromagnetic ratio is no longer constant in the static limit. Instead it decreases monotonically with increasing  $q$ , Eq.(82). As the dilaton coupling constant  $h$  is increased, the boundary curves of the domain of  $g$ , approach each other, until at the Kaluza-Klein value  $h_{\text{KK}}$  both curves coincide, as seen in Eq. (35). Considering the gyromagnetic ratio  $g$  versus  $q$ , all KK black holes fall on a single curve with  $3 \geq g \geq 2$ .

For  $h > h_{\text{KK}}$ , the boundary curves formed by the extremal and the ‘static’ black holes separate again, retaining common end points. In all cases, however, the static value of  $g$  for a given  $q$  is a rather good approximation for the true value, which becomes exact in the KK case.

The horizon electrostatic potential  $\Phi_{\text{H}}$  is shown in Fig. 4(d). As always, the static and the extremal solutions form the boundaries for the admissible values of this quantity. Analogous to the case of the gyromagnetic ratio, the two boundary curves are always rather close to each other. They approach each other with increasing  $h$ , form a single curve for the Kaluza-Klein value  $h_{\text{KK}}$  and then separate again. Thus the static value of  $\Phi_{\text{H}}$  for a given  $q$  approximates the true value well, and becomes exact in the KK case.

The scaled surface gravity  $\bar{\kappa}$  vanishes for the extremal solutions. The curves seen in Fig. 4(e) thus represent the upper boundary of the domain of existence, formed by the static solutions for the various values of the dilaton coupling  $h$ . Of particular interest is the extremal endpoint of these static curves. For  $h < h_{\text{cr}} = \sqrt{2/3}$  the surface gravity is zero at the endpoint. At the critical value  $h = h_{\text{cr}}$  the surface gravity assumes a finite value,  $\kappa_{\text{cr}}$ , whereas for  $h > h_{\text{cr}}$  the surface gravity diverges at the endpoint [36, 45]. Thus for the set of extremal rotating black holes the surface gravity jumps from zero, its value for finite angular momentum, to the finite value  $\kappa_{\text{cr}}$  for  $h = h_{\text{cr}}$  and to infinity for  $h > h_{\text{cr}}$  in the static limit, as indicated in the figure.

The figure for the scaled horizon angular velocity  $\bar{\Omega}$ , shown in Fig. 4(f), looks

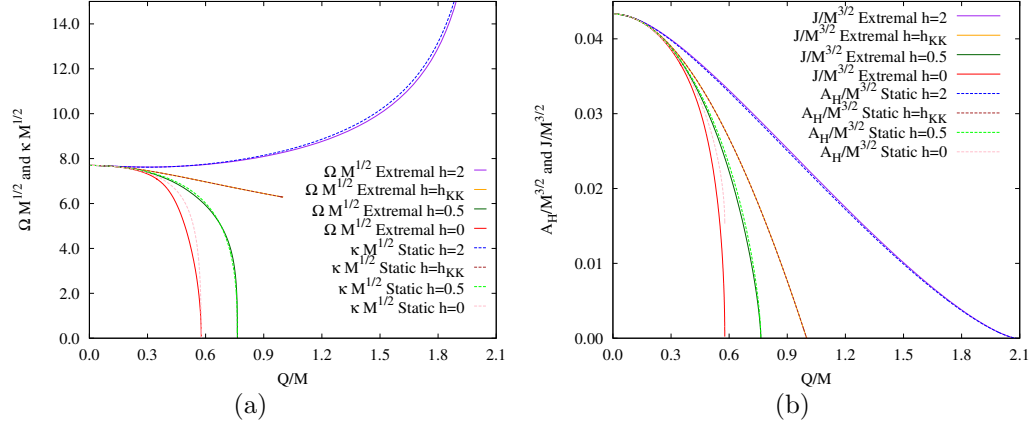


Figure 6: Properties of EMD black hole solutions in five dimensions are shown for several values of the dilaton coupling constant  $h$ :  $h = 0$  (EM),  $0.5$ ,  $\sqrt{2/3}$  (KK),  $2$ . (a) The scaled surface gravity  $\bar{\kappa} = \kappa M^{1/2}$  of the static solutions and the scaled horizon angular velocity  $\bar{\Omega} = \Omega M^{1/2}$  of the extremal solutions versus the scaled charge  $q = |Q|/M$ , (b) the scaled area  $a_H = A_H/M^{3/2}$  of the static solutions and the scaled angular momenta  $j = J/M^{3/2}$  of the extremal solutions.

completely analogous to the one for the scaled surface gravity. However, here the static solutions form the lower boundary of the domain of existence, since they have  $\Omega = 0$ , while the upper boundary is formed by the extremal rotating solutions. Inspecting again the endpoint of the set of extremal solutions, we note the same dependence on  $h$ . For  $h < h_{cr} = \sqrt{2/3}$  the horizon angular velocity vanishes at the endpoint. At the critical value  $h = h_{cr}$  the horizon angular velocity assumes a finite value,  $\Omega_{cr}$ , whereas for  $h > h_{cr}$  the horizon angular velocity diverges at the endpoint.

To better understand this analogy, let us inspect Fig. 6(a), where we compare the scaled surface gravity  $\bar{\kappa}$  of the static solutions to the scaled horizon angular velocity  $\bar{\Omega}$  of the extremal solutions for several values of the dilaton coupling  $h$ . We note, that they agree for  $h = h_{KK}$ , while they are close for other values of  $h$ . The situation is analogous, when we compare the scaled area  $a_H$  of the static solutions to the scaled angular momenta  $j$  of the extremal solutions, as seen in Fig. 6(b).

We now recall our discussion in section 3.2. There we showed, that for KK black holes in five dimensions the scaled surface gravity of static black holes indeed agrees with the scaled horizon angular velocity of extremal black holes. Considering the scaled Smarr formula, we furthermore showed relation Eq. (51) for KK black holes, which derived from the fact, that for KK black holes the horizon electrostatic potential only depends on the scaled charge. Since we have seen, that the horizon electrostatic potential depends only little on the angular momenta also for other values of the dilaton coupling  $h$ , we conclude that relation Eq. (51) holds approximately also for other values of  $h$ . This then leads to the similarity of the static  $\bar{\kappa}$  and the extremal  $\bar{\Omega}$ , as well as the similarity of the static  $a_H$  and the extremal  $j$ , observed in Figs. 6. We conclude, that we

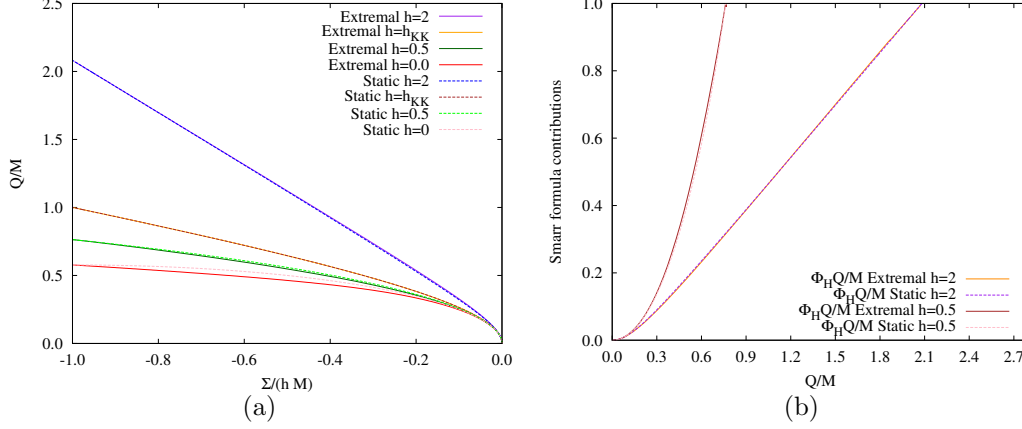


Figure 7: (a) The scaled charge  $q = Q/M$  versus the scaled relative dilaton charge  $\Sigma/(hM)$  for static and extremal solutions with  $h = 0, 0.5, h_{KK}$  and 2. The quadratic relation Eq. (96) between both scaled charges is fulfilled for every value of  $h$  in the static case, and for  $h_{KK}$  Eq. (29) in the extremal case. (b) Contributions to the Smarr formula Eq. (27) for static and extremal solutions, for both  $h = 0.5$  and  $h = 2$ .

can learn much about extremal rotating solutions by only inspecting static solutions.

In Fig. 7(a) we show the scaled charge  $Q/M$  versus the scaled relative dilaton charge  $\Sigma/(hM)$  for static and extremal solutions and several values of the dilaton coupling. Note that the quadratic relation Eq. (29) is only fulfilled in the KK case, while the static solutions satisfy a similar quadratic relation,

$$\frac{Q^2}{M + \left[1 - \frac{2(D-2)h^2}{D-3}\right] \frac{\Sigma}{2h}} = -\frac{D-3}{D-2} \frac{\Sigma}{h}, \quad (96)$$

valid for arbitrary  $h$ . It is interesting to note that this relation coincides with the quadratic relation Eq. (29) of the KK solution, when  $h = h_{KK}$ . In Fig. 7(a) we see that for extremal solutions with general dilaton coupling, this quadratic relation is almost fulfilled: the extremal curves of Fig. 7(a) are very close to the static curves, where relation Eq. (96) holds exactly. The approximation of the (in general unknown) extremal relation by the static quadratic relation is very good for large dilaton couplings (and exact in the KK case).

In Fig. 7(b) we present the Smarr formula contributions for the extremal and static solutions. Here the situation is similar. Again we note that the extremal and static curves are very close, and we can use the information from the static solutions to gain insight on the extremal solutions.

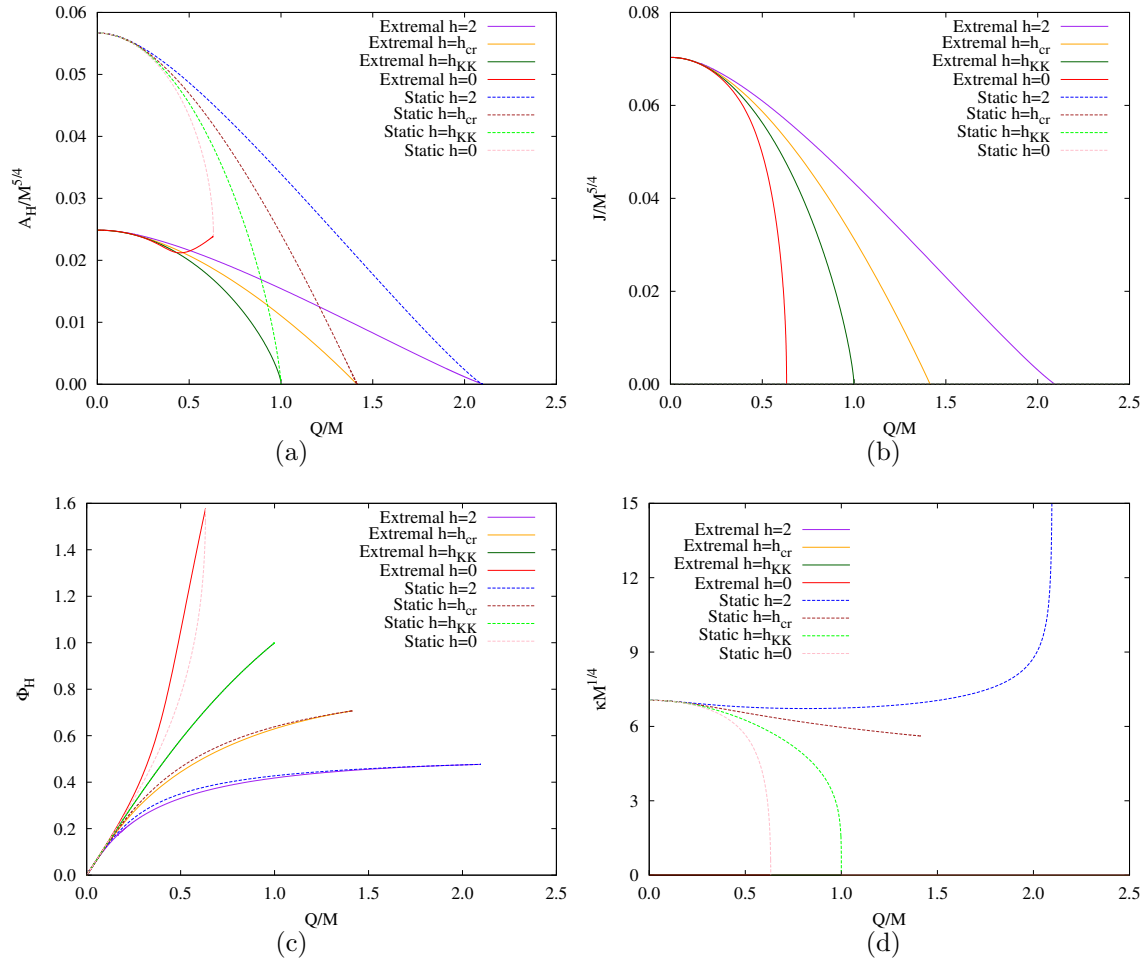


Figure 8: Properties of EMD black hole solutions in seven dimensions are shown for several values of the dilaton coupling constant  $h$ :  $h = 0$  (EM),  $h_{KK} = \sqrt{3/5}$ ,  $h_{cr} = \sqrt{8/5}$ , and  $h = 2$ . (a) The scaled area  $a_H = A_H/M^{5/4}$  versus the scaled charge  $q = |Q|/M$  for extremal and for static solutions, providing the boundary of the domain of existence. For the same sets of (extremal and static) solutions we exhibit in (b) the scaled angular momenta  $j = J/M^{5/4}$  versus  $q$ , (c) the horizon electrostatic potential  $\Phi_H$  versus  $q$ , (d) the scaled surface gravity  $\bar{\kappa} = \kappa M^{1/4}$  versus  $q$ .

## 5.4 $D > 5$

Let us now turn to black holes in more than five dimensions. Here we show, that the basic features observed for EMD black holes with equal-magnitude angular momenta are retained in higher odd dimensions. To exhibit the dependence on the number of dimensions  $D$ , we compare sets of solutions in  $D = 5, 7$ , and 9 dimensions.

### 5.4.1 $D = 7$

Let us first address the domain of existence again and recall, that unlike the case of a single non-vanishing angular momentum, where no extremal solutions exist in  $D > 5$  dimensions [1], extremal solutions always exist for odd  $D$  black holes with equal-magnitude angular momenta.

To study the dependence of these black holes on the dilaton coupling constant  $h$ , we again consider several fixed values of  $h$ :  $h = 0$ , corresponding to the EM case,  $h_{\text{KK}} = \sqrt{3/5}$ , corresponding to the KK case,  $h_{\text{cr}} = \sqrt{8/5}$ , corresponding to the critical case of the surface gravity and the horizon angular momentum, and finally  $h = 2$ .

We exhibit a number of interesting properties of these black hole solutions in Figs. 8. In particular, we show the extremal and the static solutions, which form the boundary of the domain of existence for these seven-dimensional black holes, while all non-extremal rotating black holes are located inside this boundary. The quantities shown are the scaled horizon area  $a_{\text{H}}$  (Fig. 8(a)), the scaled angular momenta  $j$  (Fig. 8(b)), the horizon electrostatic potential  $\Phi_{\text{H}}$  (Fig. 8(c)), and the scaled surface gravity  $\bar{\kappa}$  (Fig. 8(d)).

We note, that the scaled horizon area  $a_{\text{H}} = A_{\text{H}}/M^{5/4}$  is proportional to the scaled angular momenta, as long as  $h$  is non-vanishing. For  $h = 0$ , we find again the two-branch structure of the extremal EM solutions, where only the first part of the near-horizon MP branch and the second part of the near-horizon RN branch are realized globally. For the EMd solutions again the surfaces of near-horizon solutions are reduced to single curves, that are - in part - realized globally, for arbitrary non-vanishing value of the dilaton coupling  $h$ .

The gyromagnetic ratio  $g$  of these black holes attains the perturbative value  $g_{\delta q} = 5$  [10] for small values of  $q$ , independent of the dilaton coupling constant  $h$ . In all cases the ‘static’ value  $g_{\delta j}$ , Eq. (82), is a rather good approximation for the true value, which becomes exact in the KK case. Likewise, for the horizon electrostatic potential  $\Phi_{\text{H}}$  the static value for a given  $q$  approximates the true value well, and becomes exact in the KK case.

The scaled surface gravity  $\bar{\kappa} = \kappa M^{1/4}$  of the static solutions forms the upper boundary of the domain of existence, while the scaled surface gravity of the extremal solutions vanishes. At the extremal endpoints of the static curves the surface gravity is zero for  $h < h_{\text{cr}} = \sqrt{8/5}$ . This includes the KK case in seven dimensions, where  $h_{\text{KK}} = \sqrt{3/5}$ . At the critical value  $h = h_{\text{cr}}$  the surface gravity assumes a finite value,  $\kappa_{\text{cr}}$ , and for  $h > h_{\text{cr}}$  the surface gravity diverges at the endpoint [36, 45].

As discussed in five dimensions, the situation is analogous for the scaled horizon angular velocity  $\bar{\Omega}$  (not shown in the figure). Only here the static solutions form the lower boundary of the domain of existence, since they have  $\Omega = 0$ , while the upper boundary is formed by the extremal rotating solutions.

Again, we can understand this analogy by recalling our formulae in section 3.2. There we showed, that for KK black holes in  $D$  dimensions the scaled surface gravity of static black holes is proportional to the scaled horizon angular velocity of extremal black holes. We furthermore showed relation Eq. (51) for KK black holes, which derived

from the fact, that for KK black holes the horizon electrostatic potential only depends on the scaled charge.

Since the horizon electrostatic potential depends only little on the angular momenta also for other values of the dilaton coupling  $h$  in seven dimensions, relation Eq. (51) holds approximately also for other values of  $h$ . The similarity of the static  $\bar{\kappa}$  and the extremal  $\bar{\Omega}$ , as well as the similarity of the static  $a_H$  and the extremal  $j$  thus also holds in seven dimensions. Again we conclude, that we can learn much about extremal rotating solutions from the static solutions.

#### 5.4.2 $D$ -dependence

The solutions in nine dimensions do not reveal any unexpected behavior, but repeat the pattern observed in five and seven dimensions. Here the special values of the dilaton coupling constant beside the EM case  $h = 0$ , are the KK case  $h_{\text{KK}} = \sqrt{4/7}$ , known analytically, and the critical case  $h_{\text{cr}} = \sqrt{18/7}$ . As in lower dimensions, for  $h = h_{\text{cr}}$  the surface gravity of the static solutions and the horizon angular velocity of the extremal rotating solutions remain finite at  $q_{\text{max}}$ , while they diverge at  $q_{\text{max}}$  for  $h > h_{\text{cr}}$ , and tend to zero at  $q_{\text{max}}$  for  $h < h_{\text{cr}}$ .

We compare the solutions in five, seven, and nine dimensions in Figs. 9. In particular, we exhibit the EM case ( $h = 0$ ) in the left column and a generic value of the EMd case ( $h = 2$ ) in the right column.

The scaled area  $a_H = A_H/M^{(D-2)/(D-3)}$  of the extremal and static EM solutions is shown in Fig. 9(a), enclosing the domain of existence of the respective sets of black holes. For the extremal solutions it again reveals the two-branch structure, as indicated by the asterisks. As before, the near-horizon solutions are only partly realized globally. The horizon area of the EM solutions is always finite. For the EMd solutions the angular momenta and the horizon area are proportional for all extremal solutions. A single branch of near-horizon solutions is - in part - realized globally. The horizon area of EMd solutions vanishes in the extremal static case.

The gyromagnetic ratio  $g$  of these black holes attains the perturbative value  $g_{\delta q} = D - 2$  [10] for small  $q$ , independent of the dilaton coupling constant  $h$ . This indicates already, that  $g$  increases with increasing dimension  $D$ . For a given  $q$  the ‘static’ value  $g_{\delta j}$ , Eq. (82), is a rather good approximation for the true value, that becomes exact for  $h_{\text{KK}}$ . For the EM case  $g_{\delta q} = D - 3$  is a rather good approximation in general.

The horizon electrostatic potential  $\Phi_H$  (not shown in Figs. 9), is remarkably independent of the dimension  $D$ , as may be expected from its KK expression, Eq. (40). It is significantly influenced only by the dilaton coupling  $h$ . Since its dependence on the angular momenta is small, the horizon electrostatic potential found in the static limit for a given value of  $q$  represents a rather good approximation for the horizon electrostatic potential, which becomes exact in the KK case.

The scaled surface gravity  $\bar{\kappa} = \kappa M^{1/(D-3)}$  is exhibited in Figs. 9(e) and 9(f). Here the static black holes form the upper boundary of the domain of existence, while the extremal rotating black holes have vanishing  $\bar{\kappa}$ . At the extremal endpoints of the static



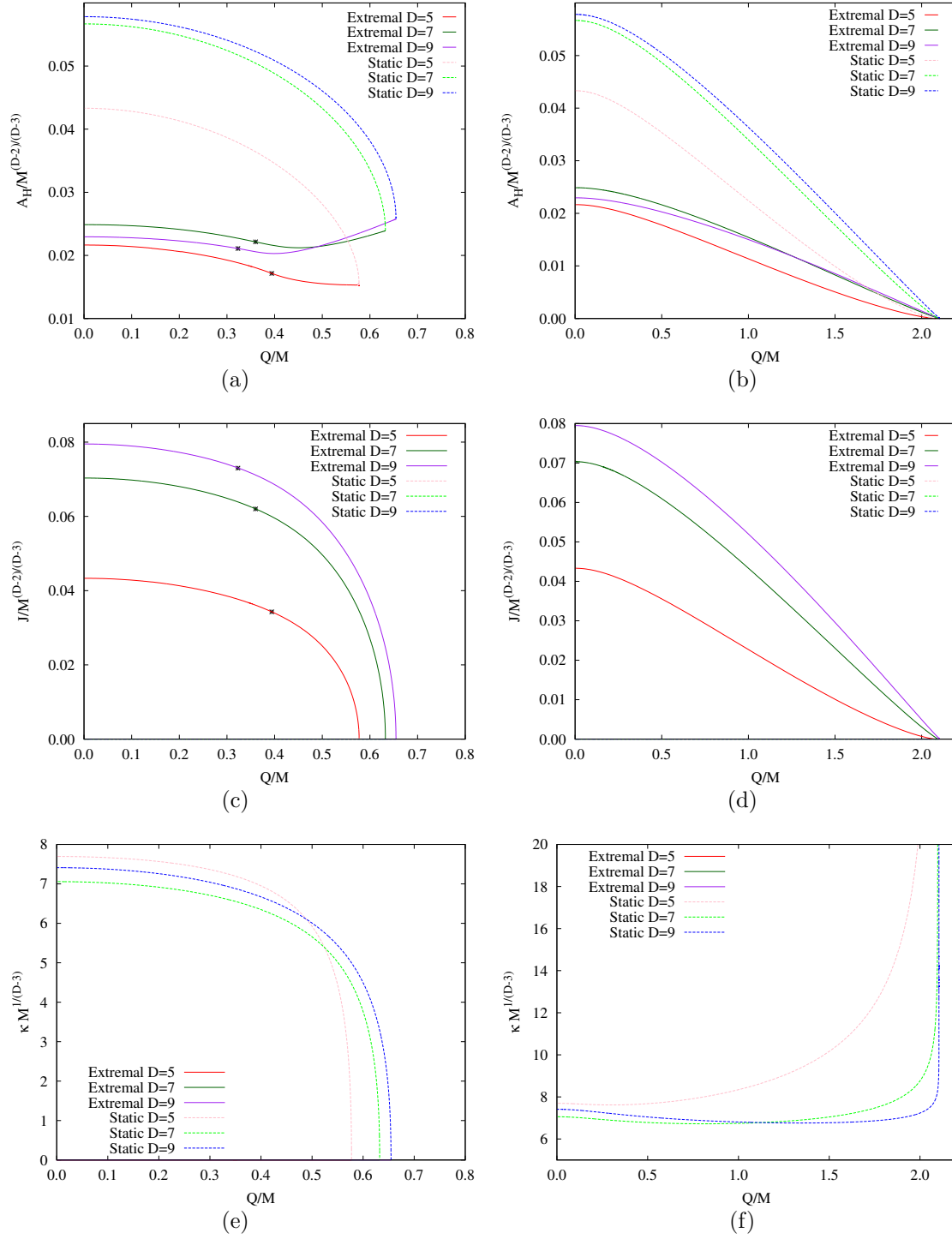


Figure 9: Properties of EMd black hole solutions in five, seven, and nine dimensions are shown for the EM case ( $h = 0$ ) (left column) and one example of the EMd case ( $h = 2$ ) (right column). The scaled area  $a_H = A_H/M^{(D-2)/(D-3)}$  versus the scaled charge  $q = |Q|/M$  (a) for  $h = 0$  and (b) for  $h = 2$  for extremal and for static solutions, providing the boundary of the domain of existence. For the same sets of solutions we exhibit the scaled angular momenta  $j = J/M^{(D-2)/(D-3)}$  versus  $q$ , (c) for  $h = 0$  and (d) for  $h = 2$ , and the scaled surface gravity  $\mathfrak{R}\mathfrak{S} = \kappa M^{1/(D-3)}$  versus  $q$  (e) for  $h = 0$  and (f) for  $h = 2$ . The asterisks mark the matching points of the two EM branches.

curves the surface gravity is zero for  $h < h_{\text{cr}}$ , corresponding to the EM case. At the critical value  $h = h_{\text{cr}}$  the surface gravity assumes a finite value,  $\kappa_{\text{cr}}$ . For  $h > h_{\text{cr}}$  the surface gravity diverges at the endpoint, as seen for the EMd case,  $h = 2$ .

The scaled horizon angular velocity  $\bar{\Omega} = \Omega M^{1/(D-3)}$  (not shown in Figs. 9) shows an analogous critical behavior, where the static and the extremal rotating solutions have switched roles. Here the extremal rotating black holes form the upper boundary of the domain of existence, while the static black holes have vanishing  $\bar{\Omega}$ . For any dimension the scaled horizon angular velocity of the extremal rotating black holes can be inferred to good approximation from the scaled surface gravity of the static black holes.

## 6 Conclusions

We have considered rotating black holes in Einstein-Maxwell-dilaton theory, which are asymptotically flat, and possess a spherical horizon topology. Restricting to odd dimensions,  $D = 2N + 1$ , and angular momenta with equal-magnitude,  $J = |J_i|$ ,  $i = 1, \dots, N$ , the symmetry of the solutions is enhanced, and the resulting cohomogeneity-1 problem is more amenable to approximate analytical treatment and to numerical analysis.

Treating the dilaton coupling constant  $h$  as a parameter, we have studied the dependence of these solutions on  $h$ . Global analytical solutions for these rotating charged black holes are only available in the Kaluza-Klein case. For extremal solutions, however, the near-horizon formalism can be employed to obtain exact solutions, describing a rotating squashed  $AdS_2 \times S^{D-2}$  spacetime. These near-horizon solutions are then interpreted as the neighborhood of the event horizon of extremal black holes.

In the EM case, we found two sets of near-horizon solutions for all odd dimensions. Denoting them as the MP branch and the RN branch, since they start at the extremal MP solution and the extremal RN solution, respectively, we noted that the solutions on the MP branch possess proportionality of the angular momenta and the horizon area, whereas the solutions on the RN branch do not. Instead these exhibit proportionality of the angular momenta and the horizon angular momenta.

Interestingly, the branches cross at a critical point, which we denoted as the matching point. Numerical construction of the extremal solutions then revealed, that only parts of these near-horizon solutions are realized globally. The sets of global solutions consists of the first part of the MP branch, reaching up to the matching point, and the second part of the RN branch, starting from the matching point.

For the EMd solutions, on the other hand, we found a single set of near-horizon solutions. But because of the presence of the dilaton field this set depends on one more parameter. However, this parameter can be eliminated by rescaling, so the physical dependence reduces to two independent parameters. Nevertheless, as in the pure EM case, analytical treatment of the extremal KK solutions and numerical construction of the extremal solutions for other values of  $h$  have revealed that there are near-horizon solutions that are not realized globally. All extremal EMd solutions possess propor-

tionality of the angular momenta and the horizon area.

We have studied the physical properties of these black holes numerically, in particular, their global charges and horizon properties. The scaling symmetry Eqs. (25)-(26) of the solutions has allowed us to give a comprehensive account of all physical properties, by scaling these quantities with the appropriate powers of the mass  $M$  or angular momentum  $J$ .

For a given dimension  $D$  and dilaton coupling constant  $h$ , any considered physical property of the corresponding family of black holes then has a domain of existence, which is determined by the set of static black holes on the one hand, and the set of extremal rotating black holes on the other hand. A generic non-extremal rotating black hole will be found within this domain of existence, whereas outside this domain singular solutions or no solutions at all should be found.

Addressing some properties, in particular, we note that the gyromagnetic ratio  $g$  increases with increasing dimension  $D$ . For the EM case  $g = D - 3$  is a rather good approximation in general, while in the EMD case, the gyromagnetic ratio can depend strongly on the scaled charge  $q$ . But the ‘static’ value, obtained perturbatively in the limit  $J \rightarrow 0$ , is a rather good approximation, that becomes exact for  $h_{\text{KK}}$ .

The horizon electrostatic potential  $\Phi_{\text{H}}$ , on the other hand, is remarkably independent of the dimension  $D$ . It is significantly influenced only by the dilaton coupling  $h$ . The static limit for a given  $q$  also represents a rather good approximation for the horizon electrostatic potential.

For the scaled surface gravity  $\bar{\kappa} = \kappa M^{1/(D-3)}$  the static black holes form the upper boundary of the domain of existence, while the extremal rotating black holes have vanishing  $\bar{\kappa}$ . At the extremal endpoints of the static curves the surface gravity is zero for  $h < h_{\text{cr}}$ . At the critical value  $h = h_{\text{cr}}$  the surface gravity assumes a finite value,  $\kappa_{\text{cr}}$ , and for  $h > h_{\text{cr}}$  the surface gravity diverges at the endpoint.

For the scaled horizon angular velocity  $\bar{\Omega} = \Omega M^{1/(D-3)}$ , on the other hand, the extremal rotating black holes form the upper boundary of the domain of existence, while the static black holes have vanishing  $\bar{\Omega}$ . Interestingly, the scaled horizon angular velocity of the extremal rotating black holes can be inferred to good approximation from the scaled surface gravity of the static black holes.

While this relation between the scaled horizon angular velocity and the scaled surface gravity is exact in the KK case, for general  $h$  it can be seen to arise from the Smarr law, the low dependence of the horizon electrostatic potential on the angular momenta, and the closeness of the horizon area of the static solutions to the angular momenta of the extremal rotating solutions. The surprising finding here is thus, that one can learn much about the extremal rotating solutions from the much simpler static solutions.

We note, that in four dimensions analogous relations hold, when the extremal and the static black hole solutions of EM theory are considered, i.e., the extremal Kerr-Newman (KN) and the static RN solutions, or the KK black holes of  $4D$  EMD theory. We conjecture, that these observations hold also for general dilaton coupling  $h$ . Since these EMD black holes represent a cohomogeneity-2 problem, we have not yet performed the corresponding numerical calculations to obtain the extremal solutions for general

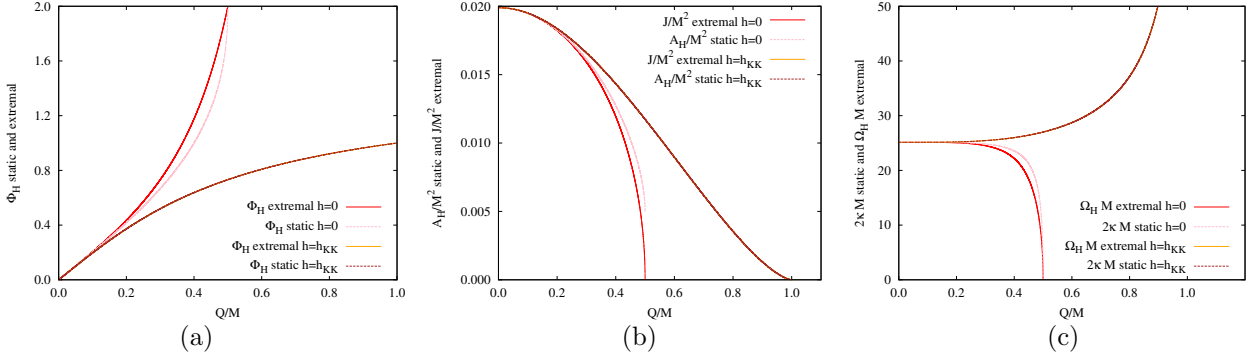


Figure 10: Properties of EMd black hole solutions in four dimensions are shown for the values of the dilaton coupling constant  $h$ :  $h = 0$  (EM),  $3/\sqrt{2}$  (KK). The horizon electrostatic potential  $\Phi_H$  of the extremal and static solutions (a), the scaled horizon area  $a_H = A_H/M^2$  of the static solutions and the scaled angular momentum  $j = J/M^2$  of the extremal solutions (b), and the scaled surface gravity  $\bar{\kappa} = \kappa M$  of the static solutions and the scaled horizon angular velocity  $\bar{\Omega} = \Omega M$  (c) versus the scaled charge  $q = |Q|/M$ .

$h$ .

Fig. 10(a) shows, that the electrostatic potential is rather independent of the angular momentum, also for the four-dimensional EM case, while the KK solutions again have no dependence on the angular momentum. Moreover, for a given scaled charge, the scaled horizon area of the static RN solutions is very close to the scaled angular momentum of the extremal KN solutions, as long as the scaled charge is not too close to its maximal value, as seen in Fig. 10(b). For the KK solutions, on the other hand, the scaled horizon area of the static solutions and the extremal solutions is identical.

Consequently, it follows from the Smarr relation in four dimensions that the scaled surface gravity of the static RN solutions is very close to one-half of the scaled horizon angular velocity of the extremal KN solutions. This is illustrated in Fig. 10(c). For the KK solutions the relation  $2\bar{\kappa}_{st} = \bar{\Omega}_{ex}$  holds exactly, and we expect that this relation should hold approximately for all values of the dilaton coupling.

Concerning the near-horizon geometry, in [39] four-dimensional Kaluza-Klein black holes are studied. However, these solutions possess both electric and magnetic charge [35, 46]. Interestingly, here (for fixed magnetic charge) also two branches of black holes are present: the ergo-free branch, which connects to the static RN solution, and the ergo branch, which connects to the extremal Kerr solution.

The near-horizon geometry of the ergo-free branch is independent of the particular value of the dilaton at infinity, therefore this branch represents an attractor. In contrast, the near-horizon geometry of the ergo branch does depend on the value of the dilaton at infinity and so does the value of the dilaton at the horizon. Of course, for a given angular momentum and charge all these solutions are equivalent under the scaling

symmetry. But the scaling relation depends on the asymptotic value of the dilaton.

This property of the ergo branch of four-dimensional EMd black holes is similar to what we have found for the branch of extremal EMd black holes in odd  $D$ -dimensions, where the geometry at the horizon also depends on the asymptotic value of the dilaton at infinity. But since the area is proportional to the total angular momentum, if the total angular momentum is fixed, the attractor mechanism works and the entropy does not depend on the value of the dilaton at infinity. We plan to investigate these four-dimensional EMd solutions further, allowing for general values of the dilaton coupling constant [46].

Another case of interest in this connection is represented by the black holes of Einstein-Maxwell-Chern-Simons (EMCS) theory [47, 48, 49, 50, 51]. In the supergravity case, these black holes are known analytically. The extremal black holes then again exhibit two branches, an ergo-free branch and an ergo branch. When the Chern-Simons (CS) coupling constant is increased beyond the supergravity value, one of the branches of extremal black holes becomes counterrotating. When the CS coupling constant is increased even further, beyond a critical value further branches of extremal black holes arise.

Comparing these global EMCS solutions to near-horizon solutions, one realizes that the relation between global solutions and near-horizon solutions becomes even more diverse than observed in EMd theory. In particular, such an EMCS near-horizon solution can correspond to i) more than one global solution, ii) precisely one global solution, or iii) no global solution at all. Clearly, only a study of near-horizon solutions is insufficient to clarify the domain of existence of extremal solutions. Thus the construction of the global solutions is indeed essential, as was first observed for the extremal dyonic black holes of  $D = 4$  Gauß-Bonnet gravity [52].

## Acknowledgment

We would like to thank J. Viebahn for initial collaboration on this project, and B. Kleihaus and E. Radu for helpful discussions. We gratefully acknowledge support by the Spanish Ministerio de Ciencia e Innovacion, research project FIS2011-28013, and by the DFG, in particular, the DFG Research Training Group 1620 “Models of Gravity”. J. L. B.-S. was supported by the Spanish Universidad Complutense de Madrid.

## References

- [1] R. C. Myers and M. J. Perry, *Annals Phys.* **172**, 304 (1986).
- [2] R. C. Myers, arXiv:1111.1903 [gr-qc].
- [3] D. Youm, *Phys. Rept.* **316**, 1 (1999) [arXiv:hep-th/9710046].
- [4] K. -i. Maeda and M. Nozawa, *Prog. Theor. Phys. Suppl.* **189**, 310 (2011) [arXiv:1104.1849 [hep-th]].

- [5] D. Marolf, arXiv:1107.1022 [hep-th].
- [6] A. Chodos and S. L. Detweiler, Gen. Rel. Grav. **14**, 879 (1982).
- [7] V. P. Frolov, A. I. Zelnikov and U. Bleyer, Annalen Phys. **44**, 371 (1987).
- [8] J. H. Horne and G. T. Horowitz, Phys. Rev. D **46**, 1340 (1992) [hep-th/9203083].
- [9] J. Kunz, D. Maison, F. Navarro-Lérida and J. Viebahn, Phys. Lett. B **639**, 95 (2006) [hep-th/0606005].
- [10] A. N. Aliev and V. P. Frolov, Phys. Rev. D **69**, 084022 (2004) [arXiv:hep-th/0401095].
- [11] A. N. Aliev, Mod. Phys. Lett. A **21**, 751 (2006) [arXiv:gr-qc/0505003].
- [12] A. N. Aliev, Phys. Rev. D **74**, 024011 (2006) [arXiv:hep-th/0604207].
- [13] F. Navarro-Lérida, Gen. Rel. Grav. **42**, 2891 (2010) [arXiv:0706.0591 [hep-th]].
- [14] A. Sheykhi, M. Allahverdizadeh, Y. Bahrampour and M. Rahnama, Phys. Lett. B **666**, 82 (2008) [arXiv:0805.4464 [hep-th]].
- [15] M. Allahverdizadeh, J. Kunz and F. Navarro-Lérida, Phys. Rev. D **82**, 024030 (2010) [arXiv:1004.5050 [gr-qc]].
- [16] M. Allahverdizadeh, J. Kunz and F. Navarro-Lérida, Phys. Rev. D **82**, 064034 (2010) [arXiv:1007.4250 [gr-qc]].
- [17] J. Kunz, F. Navarro-Lérida and A. K. Petersen, Phys. Lett. B **614**, 104 (2005) [arXiv:gr-qc/0503010].
- [18] J. Kunz, F. Navarro-Lérida and J. Viebahn, Phys. Lett. B **639**, 362 (2006) [arXiv:hep-th/0605075].
- [19] J. L. Blázquez-Salcedo, J. Kunz and F. Navarro-Lérida, arXiv:1309.2088 [gr-qc].
- [20] M. Cvetič, G. W. Gibbons and C. N. Pope, Phys. Rev. Lett. **106**, 121301 (2011) [arXiv:1011.0008 [hep-th]].
- [21] M. Ansorg and H. Pfister, Class. Quant. Grav. **25**, 035009 (2008) [arXiv:0708.4196 [gr-qc]].
- [22] J. Hennig, M. Ansorg and C. Cederbaum, Class. Quant. Grav. **25**, 162002 (2008) [arXiv:0805.4320 [gr-qc]].
- [23] M. Ansorg and J. Hennig, Class. Quant. Grav. **25**, 222001 (2008) [arXiv:0810.3998 [gr-qc]].

- [24] J. Hennig, C. Cederbaum and M. Ansorg, Commun. Math. Phys. **293**, 449 (2010) [arXiv:0812.2811 [gr-qc]].
- [25] M. Ansorg and J. Hennig, Phys. Rev. Lett. **102**, 221102 (2009) [arXiv:0903.5405 [gr-qc]].
- [26] J. Hennig and M. Ansorg, Annales Henri Poincare **10**, 1075 (2009) [arXiv:0904.2071 [gr-qc]].
- [27] M. Ansorg, J. Hennig and C. Cederbaum, Gen. Rel. Grav. **43**, 1205 (2011) [arXiv:1005.3128 [gr-qc]].
- [28] A. Castro and M. J. Rodríguez, Phys. Rev. D **86**, 024008 (2012) [arXiv:1204.1284 [hep-th]].
- [29] S. S. Yazadjiev, Phys. Rev. D **87**, 024016 (2013) [arXiv:1210.4684 [gr-qc]].
- [30] S. Yazadjiev, Class. Quant. Grav. **30**, 115010 (2013) [arXiv:1301.1548 [hep-th]].
- [31] J. P. Gauntlett, R. C. Myers and P. K. Townsend, Class. Quant. Grav. **16**, 1 (1999) [arXiv:hep-th/9810204].
- [32] B. Kleihaus, J. Kunz and F. Navarro-Lérida, Phys. Rev. Lett. **90**, 171101 (2003) [arXiv:hep-th/0210197].
- [33] P. M. Llatas, “Electrically Charged Black-holes for the Heterotic String Compactified on a Phys. Lett. B **397**, 63 (1997) [arXiv:hep-th/9605058].
- [34] G. W. Gibbons and D. L. Wiltshire, Annals Phys. **167**, 201 (1986) [Erratum-ibid. **176**, 393 (1987)].
- [35] D. Rasheed, Nucl. Phys. B **454**, 379 (1995) [arXiv:hep-th/9505038].
- [36] G. W. Gibbons and K. -i. Maeda, Nucl. Phys. B **298**, 741 (1988).
- [37] D. Garfinkle, G. T. Horowitz and A. Strominger, Phys. Rev. D **43**, 3140 (1991) [Erratum-ibid. D **45**, 3888 (1992)].
- [38] R. Gregory and J. A. Harvey, Phys. Rev. D **47**, 2411 (1993) [arXiv:hep-th/9209070].
- [39] D. Astefanesei, K. Goldstein, R. P. Jena, A. Sen and S. P. Trivedi, JHEP **0610** (2006) 058 [arXiv:hep-th/0606244].
- [40] K. Goldstein and R. P. Jena, JHEP **0711** (2007) 049 [arXiv:hep-th/0701221].
- [41] H. K. Kunduri and J. Lucietti, arXiv:1306.2517 [hep-th].
- [42] B. Kleihaus and J. Kunz, Phys. Rev. Lett. **86**, 3704 (2001) [arXiv:gr-qc/0012081].

- [43] U. Ascher, J. Christiansen, R. D. Russell, Mathematics of Computation 33 (1979) 659; ACM Transactions 7 (1981) 209.
- [44] S. Yazadjiev, JHEP **1106**, 083 (2011) [arXiv:1104.0378 [hep-th]].
- [45] G. T. Horowitz and A. Strominger, Nucl. Phys. B **360**, 197 (1991).
- [46] B. Kleihaus, J. Kunz and F. Navarro-Lérida, Phys. Rev. D **69**, 081501 (2004) [gr-qc/0309082].
- [47] J. C. Breckenridge, R. C. Myers, A. W. Peet and C. Vafa, Phys. Lett. B **391**, 93 (1997) [arXiv:hep-th/9602065].
- [48] M. Cvetič, H. Lu and C. N. Pope, Phys. Lett. B **598**, 273 (2004) [arXiv:hep-th/0406196].
- [49] Z. W. Chong, M. Cvetič, H. Lu and C. N. Pope, Phys. Rev. Lett. **95**, 161301 (2005) [arXiv:hep-th/0506029].
- [50] J. Kunz and F. Navarro-Lérida, Phys. Rev. Lett. **96**, 081101 (2006) [hep-th/0510250].
- [51] J. L. Blázquez-Salcedo, J. Kunz, F. Navarro-Lérida and E. Radu, arXiv:1308.0548 [gr-qc].
- [52] C. -M. Chen, D. V. Gal'tsov and D. G. Orlov, Phys. Rev. D **78**, 104013 (2008) [arXiv:0809.1720 [hep-th]].